J Therm Spray Tech
https://doi.org/10.1007/s11666-026-02327-x

REVIEW

Thermal Spray as a Scalable Alternative Processing Route for Solid-State Thin-Film Batteries

Ameey Anupam[1] · Arman Hasani[2] · Gidla Vinay[2] · Chinmayee Nayak[2] · Nikhil Kamboj[2] · Shrikant Joshi[1] · Ashish Ganvir[2]

Submitted: 19 February 2026 / in revised form: 26 August 2026 / Accepted: 27 August 2026
© The Author(s) 2026

Abstract Solid-state thin-film batteries (SSTFBs) are attractive for applications where small footprint, safety, long cycle life, and device integration are more important than high absolute capacity. Their fabrication, however, presently remains strongly tied to vacuum-based thin-film methods such as sputtering, pulsed laser deposition, evaporation, atomic layer deposition, and chemical vapour deposition. These routes provide dense and compositionally controlled layers, but their low deposition rates, high cost, limited coating area, and difficulty in building thicker active layers restrict their wider implementation for manufacturing. Thermal spray offers a distinct and versatile processing route that can deposit metals, ceramics, and composites from powder, suspension, or solution precursor feedstocks at significantly higher rates and over larger areas. This review assesses whether thermal spray approaches can be useful for SSTFB manufacture, while also considering the strict requirements of battery layers. The discussion first summarizes SSTFB materials and conventional processing constraints associated with them, before examining the suitability of thermal spraying as a processing platform based on its inherent characteristics in terms of thermal exposure, kinetic energy, feedstock response, phase retention, and coating/interface formation. Component-level compatibility is considered separately for SSTFB anodes, cathodes, solid electrolytes, and current collectors. Recent studies demonstrate that thermally sprayed battery constituents can exhibit electrochemical functionality, but alkali ion (lithium/sodium) loss, secondary phase formation, roughness, residual porosity, interfacial reactions, contamination control, and reproducibility remain key challenges. However, a strong near-term role of thermal spray is anticipated for fabrication of selected layers, current collectors, conductive interlayers, thicker active coatings, and hybrid architectures where complementary thin-film or post-treatment steps can address interface and electrolyte-quality requirements. The review concludes by proposing benchmark comparison criteria, minimum reporting parameters, and a staged roadmap for moving towards thermal-spray-enabled SSTFB manufacturing.

Novelty Statement This review examines thermal spray from the specific viewpoint of solid-state thin-film battery manufacturing. Its main contribution is to connect SSTFB layer requirements with thermal-spray processability, indicating where thermal spray may be useful directly, where post-treatment or hybrid processing could be needed, and where conventional thin-film routes are likely to be more appropriate. The review also brings together recent thermal-spray studies on battery-relevant materials and architectures, including single-layer, interface-focussed configurations, and emerging multilayer/full-stack demonstrations, along with advanced characterization insights, benchmark manufacturing comparisons, and minimum reporting requirements to define a realistic development path for thermal-spray-enabled SSTFB layers and architectures.

Keywords solid state thin film batteries · thermal spray

Ameey Anupam and Arman Hasani share first co-authorship for this article.

✉ Ameey Anupam
ameey.anupam@hv.se

[1] Department of Engineering Science, University West, 46186 Trollhättan, Sweden

[2] DMS Research Group, Department of Mechanical and Materials Engineering, University of Turku, 20014 Turku, Finland

Published online: 23 September 2026

Introduction

Rechargeable lithium-ion batteries have enabled portable electronics, electric vehicles, and several emerging energy-storage applications. Conventionally, these have been based on liquid-electrolyte cell architectures, which face limitations related to safety, packaging flexibility, and long-term stability (Ref 1-3). All-solid-state batteries address some of these issues by replacing the liquid electrolyte and separator with a solid electrolyte, which can improve safety and allow more compact cell designs (Ref 4, 5). Within this broader class, solid-state thin-film batteries (SSTFBs) represent a more specialized architecture, where the battery components are deposited as thin, solid layers. Such a format is particularly attractive when small size, safety, long cycle life, and device integration are more important than high absolute capacity (Ref 6, 7). SSTFBs are, therefore, relevant for microelectronics, medical implants, distributed sensors, microrobots, and internet-of-things devices, where the power source must occupy a small footprint while remaining reliable over long operating periods (Ref 6, 7). Although most reported SSTFB demonstrations are based on lithium chemistries, sodium-based solid-state thin-film batteries are also being explored within the broader solid-state thin-film battery framework (Ref 8). Their interest is partly linked to the greater abundance and lower cost of sodium, although sodium-based thin-film systems remain less mature than Li-based microbatteries.

A typical SSTFB consists of a multilayer stack comprising a current collector, cathode, solid electrolyte, anode, and a second current collector, as illustrated in Fig. 1. The individual layers are typically in the sub-micrometre to few-micrometre range, providing short transport distances that are beneficial for compact device architectures (Ref 9). However, such a configuration leaves little tolerance for defects in the multilayer stack. The films must be continuous and well controlled in thickness, and the interfaces must remain chemically compatible during processing and operation (Ref 10). Thus, unlike bulk solid-state batteries, where performance is often limited by long transport paths and pressure-dependent interfaces, SSTFBs rely heavily on the ability to manufacture thin, continuous, and well-integrated multilayer stacks (Ref 11).

The main limitation of SSTFBs lies in translating laboratory-scale device fabrication into scalable, cost-effective production while maintaining the stringent material and interface requirements needed for reliable performance. Manufacturing continues to be the primary challenge. Conventional vacuum-based routes such as sputtering (Ref 12-14), pulsed laser deposition (PLD) (Ref 15, 16), and atomic layer deposition (ALD) (Ref 17, 18) can produce dense, smooth, and compositionally controlled layers and remain the dominant routes for laboratory-scale SSTFB fabrication. These techniques are particularly useful when very thin electrolytes, sharp interfaces, or conformal protective layers are required (Ref 19). Their limitations are mainly related to the processes being typically slow and expensive, and the deposition area often restricted (Ref 20). Increasing the active-layer thickness is a direct way to improve areal capacity, but it also makes film integration more difficult. Thicker cathode films are more susceptible to intrinsic, thermal, and cycling-induced stresses, which can promote cracking, surface roughening, and loss of the smooth interface quality needed for sequential SSTFB deposition (Ref 21, 22). This creates a practical limitation: the same features that make thin-film methods attractive for precision devices restrict their utility for larger-area or higher-loading architectures. Solution-based and printing methods partly address the scalability problem by improving material utilization and patterning flexibility (Ref 23, 24). However, the printed or solution-derived layer usually has to be transformed into the final dense functional film after deposition. This post-deposition conversion is often the critical step, since drying and thermal treatment can change both the film microstructure and the interface chemistry (Ref 25, 26). These constraints are not limited to Li-based SSTFBs, but also apply to emerging Na-based solid-state thin-film systems. However, because Na-based electrodes and electrolytes involve different chemistries and process windows, lessons from Li-based SSTFBs should be transferred cautiously rather than assumed directly. These considerations show that there remains a clear gap between the precision of conventional thin-film routes and the requirements of scalable manufacturing.

Thermal spray processing is potentially interesting in the context of the above shortcomings because it offers high-rate deposition of metals, ceramics, and composites from powder, suspension, or solution precursor feedstocks (Ref 27, 28). It can produce coatings over relatively large areas, with flexible thickness control and without the need for organic binders. These features make it relevant to consider thermal spray for depositing selected SSTFB layers, particularly where thicker functional coatings, higher material loading, or scalable deposition are required. At the same time, it is pertinent to acknowledge that thermal spray is not automatically compatible with all battery materials. Depending upon the material of interest, the high thermal and kinetic inputs can affect both the chemistry and the microstructure of the deposited layer. The main chemical risks are elemental loss (e.g., particularly in case of Li/Na-containing chemistries), phase decomposition, and compositional drift (Ref 29, 30). At the coating level, porosity, rough surfaces, or residual stresses could present potential

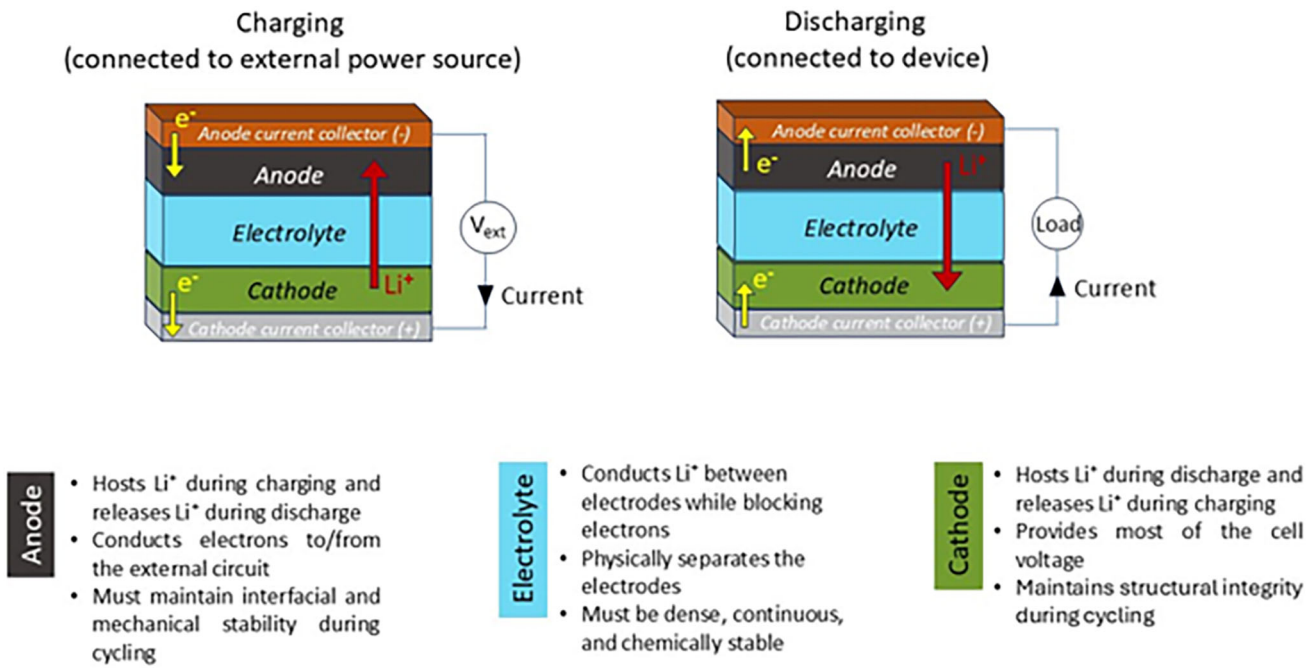

Fig. 1 Schematic representation of a solid-state thin-film battery (SSTFB), shown here for a Li-based cell during charging and discharging. During charging, Li^+ ions migrate from the cathode towards the anode under an externally applied potential, while during discharging they migrate from the anode towards the cathode as electrons flow through the external circuit. The lower panel summarizes the primary functions of the anode, solid electrolyte, and cathode layers relevant to SSTFB operation and manufacturing

challenges while the interfaces may be affected by inter-diffusion and reaction-zone formation (Ref 31, 32).

This review evaluates the opportunities and limitations of thermal spray for SSTFB manufacturing from a processing perspective. It first summarizes SSTFB materials and conventional manufacturing routes, followed by examining thermal spray process selection, possible process-induced changes in battery-relevant materials, and component-level requirements for SSTFB layers. Reported studies on thermally sprayed materials and architectures of interest to SSTFBs are reviewed in this context and compared with established fabrication routes. The final sections discuss manufacturing challenges, reporting needs, and staged research priorities for assessing thermal spray as an enabling route for SSTFB manufacturing.

Materials and Conventional Manufacturing Routes for SSTFBs

SSTFBs place stricter demands on materials processing than bulk solid-state batteries because each component has to be deposited as part of a closely integrated stack. The requirements are not only electrochemical, but also linked to layer geometry, defect tolerance, and interface formation. The solid electrolyte must be dense and continuous to prevent electronic leakage or short-circuit paths. The electrode layers, in turn, must retain sufficient crystallinity, connected transport pathways, and mechanical integrity at limited thickness (Ref 33). Reported layer dimensions are typically 0.1-10 µm for solid electrolytes, 1-10 µm for cathodes, and around 1 µm for anodes (Ref 34). At these thicknesses, even small changes in film continuity, surface roughness, residual stress, or interfacial chemistry can strongly affect cell behaviour (Ref 35, 36). Materials selection in SSTFBs is closely linked to the deposition route used to form and integrate each layer.

The need for controlled and well-integrated layers in SSTFB fabrication has been the driver for the traditional interest in vacuum-based thin-film processing. Sputtering, PLD, thermal evaporation, and molecular beam epitaxy (MBE) are commonly used to obtain dense and compositionally controlled layers, while ALD and chemical vapour deposition (CVD) are useful when conformality or interface modification is required (Ref 37). These methods differ in how the coating material is transported from the vapour phase to the substrate. Sputtering and PLD remove material from a solid target using plasma ions or laser ablation, respectively, whereas thermal evaporation relies on physical vaporization of the source material. MBE uses directed atomic or molecular beams under ultra-high vacuum, while ALD and CVD grow films through surface or vapour-phase chemical reactions. For SSTFBs, the main advantage of these routes is the high degree of control they

provide over layer thickness, composition, and interface definition. This is particularly important for electrolytes and interlayers, where pinholes, roughness, or local defects can increase resistance or create electronic leakage paths (Ref 38). In contrast, the limitations of the above thin-film approaches are mainly related to manufacturing scale. Most of these processes are slow, equipment-intensive, and less suited to deposition of thick active layers or large-area multilayer production (Ref 36).

Solution-based and printing methods provide an alternative to vacuum-based SSTFB fabrication when lower-cost, liquid-feedstock, or more scalable processing is desired. Sol–gel routes are mainly useful for oxide and composite electrolyte films because the chemistry can be adjusted at the precursor stage, followed by conversion to a ceramic or glassy layer during drying and heat treatment (Ref 39). Printing and coating methods, including screen printing, inkjet printing, spray coating, and doctor blading, instead rely on particle- or precursor-containing inks that are deposited as patterned or continuous wet layers (Ref 24, 40). Their main advantage is that material placement and layer geometry can be controlled more directly, with reduced dependence on high-vacuum infrastructure. The important point, however, is that these deposited layers are not usually functional immediately after deposition. They must be converted into solid battery layers through solvent removal and, in many cases, thermal treatment. This conversion step is often where the main processing risks appear. In sol–gel films, drying and annealing can lead to porosity, cracking, thickness variability, alkali loss, or damage to underlying layers (Ref 41, 42). In printed ceramic layers, incomplete densification can reduce ionic conductivity, while high-temperature annealing or flash sintering may promote alkali volatilization or interdiffusion between adjacent layers (Ref 43, 44).

With this conventional SSTFB-relevant processing background established, the following sections summarize the main SSTFB material classes and the conventional routes used to fabricate them, with emphasis on the processing constraints that motivate interest in alternative scalable approaches. Since the reported SSTFB literature remains largely centred on Li-based systems, the following component-wise discussion focuses primarily on Li-based materials. Sodium-based SSTFB systems are noted where relevant to acknowledge analogous anode, cathode, and electrolyte chemistries, as well as related material-integration challenges. Compared with Li-based systems, Na-based SSTFBs involve different electrode and electrolyte chemistries, larger mobile Na^+ ions, and less mature thin-film device demonstrations. Therefore, the discussion below treats Na-based materials as technologically related to Li-based SSTFBs, but not directly interchangeable with them.

Anodes

Lithium metal remains the most widely investigated anode for SSTFBs because of its high theoretical capacity and low electrochemical potential (Ref 45, 46). In thin-film cells, it is usually introduced by thermal evaporation, e-beam evaporation, sputtering, or direct lamination of rolled lithium foil (Ref 47-49). These routes can produce thin lithium layers without slurry processing, but the Li/electrolyte interface remains difficult to stabilize. The main issues are poor interfacial contact and progressive degradation during cycling. Poor wetting and high interfacial resistance can limit charge transfer, while parasitic reactions or dendrite formation can damage the interface over time (Ref 50). For this reason, lithium-metal anodes are often used together with interface modification strategies, including buffer layers, surface texturing, alloying, or protective interphases (Ref 51, 52). Lithium-alloy systems such as Li-In, Li-Al, Li-Sn, Li-Si, and Li-Ge have also been explored because they can improve wetting or interfacial stability compared with pure lithium (Ref 53-55). Some of these alloys are useful as model or reference anodes, while others are considered for improving cyclability in thin-film formats. Still, their use depends strongly on whether the film can maintain a stable interface and accommodate volume or stress evolution during cycling.

Silicon is another attractive anode material because of its high capacity and compatibility with microfabrication routes (Ref 56, 57). Thin-film deposition methods can provide good control over Si film thickness, morphology, and, in the case of Si-alloy anodes, composition. The main limitation here is mechanical stability during cycling. Silicon undergoes large volume changes during lithiation and delithiation, which can lead to cracking, loss of contact, or progressive mechanical degradation unless the layer is kept very thin or incorporated into a multilayer or composite architecture (Ref 35, 58, 59). This illustrates a broader SSTFB constraint: successful thin-film deposition does not necessarily guarantee mechanical or electrochemical stability during operation.

Materials such as graphite, titanates, and transition-metal oxides have also been explored as anodes for SSTFBs (Ref 60, 61). Lithium titanate, commonly $Li_4Ti_5O_{12}$ (LTO), is significant because it undergoes relatively small volume change during cycling compared with high-capacity alloying anodes (Ref 62). However, the relevance of these materials is limited not only by electrochemical activity, but also by how well they are translated into ultrathin deposited layers. At the thicknesses relevant to SSTFBs, it can be difficult to obtain dense and uniform films of these materials while still achieving meaningful areal capacity (Ref 36, 37). As a result, behaviour

demonstrated in bulk or composite electrodes cannot be directly assumed for thin-film architectures.

In sodium-based thin-film systems, the anode choice similarly links the charge-storage mechanism to the deposition route. Metallic Na is typically introduced by low-temperature physical deposition such as thermal evaporation, while Na-hosting anodes shift the processing challenge towards forming stable carbon-based, Ti-based insertion, or alloy-type films (Ref 63). Representative examples include hard carbon, $Na_2Ti_3O_7$ or $NaTi_2(PO_4)_3$ insertion anodes, and Sn- or Sb-based Na alloy-type anodes, which may be processed by sputtering, PLD, solution-derived processing, or related thin-film/coating routes (Ref 63, 64).

From a manufacturing viewpoint, anodes remain one of the more difficult SSTFB components to scale. Alkali-metal anodes require controlled handling and careful interface engineering because their performance is strongly affected by the quality of contact at the anode/electrolyte and anode/current-collector interfaces. Host-type or alloy-type anodes, such as Si, Li alloys, Na alloys, and selected oxide anodes like LTO avoid some of the direct alkali-metal handling, but they introduce their own processing constraints. Their thickness, microstructure, adhesion, and mechanical stability must be tightly controlled during deposition and cycling.

Cathodes

Cathode materials used in SSTFBs are largely adapted from established lithium-ion battery chemistries although sodium-based cathode families are also relevant for emerging Na-based SSTFB systems. Layered oxides such as $LiCoO_2$ (LCO), $LiNi_xMn_yCo_zO_2$ (NMC), and $LiNi_{1-x-y}Co_xAl_yO_2$ (NCA) are the most common examples, while spinel and polyanionic compounds have also been explored for high-rate or structurally stable thin-film configurations (Ref 65). For Na-based systems, representative cathode families include layered $NaMO_2$-type transition-metal oxides, Na-based polyanionic compounds such as $Na_3V_2(PO_4)_3$, and Prussian Blue or Prussian Blue analogue cathodes (Ref 66). In SSTFBs, however, the cathode cannot be selected only based on capacity or voltage. For thin-film integration, the main concerns remain crystallinity, alkali stoichiometry, phase stability, and compatibility with the adjacent solid electrolyte, especially when post-deposition treatment is needed to obtain the desired cathode structure (Ref 67). $LiCoO_2$ remains the most established cathode material for SSTFBs because of its stable thin-film processing behaviour and mature electrochemical performance (Ref 68). It is commonly deposited by sputtering, PLD, or evaporation, followed by annealing to obtain the desired crystalline structure (Ref 69, 70). Other layered oxides such as NMC, NCA and $NaMO_2$-type transition-metal oxides offer higher theoretical capacities but are more difficult to process as thin films because maintaining alkali stoichiometry and phase purity becomes increasingly challenging during deposition and annealing (Ref 71). Spinel and polyanionic cathodes offer advantages in structural stability and rate capability, but their integration into thin-film multilayer stacks is still less mature (Ref 72-74).

For cathodes, the main manufacturing challenge is that deposition and functional performance are closely linked. A film may be successfully deposited, but can still require crystallization, stoichiometry control, and interface preservation to operate as a useful cathode layer (Ref 48). Vacuum-based routes provide strong control over film thickness and composition, but their throughput and deposition area remain limited (Ref 75). Solution and printing routes offer a more scalable route, but the processing risk is shifted to the conversion step, where drying and heat treatment can affect film density, alkali retention, and compatibility with adjacent layers (Ref 76). Thus, the key question for cathodes is not only whether the material can be deposited, but whether it can be crystallized and integrated without damaging the multilayer stack. Sulphide-based cathode systems are even more difficult to incorporate into SSTFB architectures. Their air and moisture sensitivity, together with their limited compatibility with high-temperature or high-vacuum processing, restricts their use in conventional thin-film stacks (Ref 77-79). Consequently, they are viewed as exploratory systems for low-temperature, solution-based, or hybrid processing approaches rather than mature SSTFB cathode materials.

Solid Electrolytes

The solid electrolyte is one of the most processing-sensitive components in SSTFBs. It must conduct ions while blocking electronic transport, and it must do so as a thin, continuous layer within a multilayer stack (Ref 80). This requirement is more restrictive than in bulk solid-state batteries, where thicker ceramic pellets, polymer membranes, or composite separators can be used. In SSTFBs, even small defects in the electrolyte can increase leakage, raise interfacial resistance, or create short-circuit paths. Lithium phosphorus oxynitride (LiPON) remains the benchmark electrolyte for SSTFBs because it is comparatively easier to process as a reliable thin film. It is commonly deposited by radio-frequency (RF) magnetron sputtering and forms smooth, amorphous films with good stability against lithium metal (Ref 81, 82). Its ionic conductivity is lower than that of many crystalline oxide or sulphide electrolytes, but its processability and interfacial stability have made it the reference system for long-life

thin-film microbatteries (Ref 83). Typical examples of crystalline oxide electrolytes that offer higher bulk ionic conductivity, although they are more difficult to integrate into SSTFB architectures, are lithium lanthanum zirconate (LLZO) and lithium lanthanum titanate (LLTO) (Ref 23, 84, 85). Their thin films are usually prepared by PLD, sputtering, ALD, or related routes, often followed by high-temperature annealing to obtain the desired crystalline phase (Ref 15, 86). This post-treatment step is one of the main integration challenges. It can alter lithium content, promote interdiffusion, introduce thermal stress, or damage neighbouring layers. For this reason, many oxide-electrolyte studies are viewed as process-feasibility demonstrations rather than mature device-level solutions.

Sodium-based SSTFBs involve different solid-electrolyte chemistries while retaining the same basic requirement. Representative Na-ion solid electrolytes include NASICON-type oxides such as $Na_3Zr_2Si_2PO_{12}$ and β''-Al_2O_3-type electrolytes (Ref 8, 87). These materials are commonly processed through ceramic powder/sintering routes or adapted to thin-film and coating formats using methods such as sputtering, PLD, sol–gel/solution-derived processing, tape casting, or related routes (Ref 88).

Sulphide, polymer, and composite electrolytes represent alternative classes of solid electrolytes with distinct material properties and processing considerations across Li- and Na-based systems. Sulphide electrolytes provide high ionic conductivity in bulk form, but their moisture sensitivity and chemical reactivity make thin-film processing difficult (Ref 89-92). Polymer and composite electrolytes are attractive for low-temperature or flexible architectures, but their room-temperature conductivity and mechanical stability often remain limiting (Ref 93-96). Overall, electrolyte fabrication remains a central bottleneck for SSTFB manufacturing.

Current Collectors and Substrates

Current collectors and substrates serve different but closely linked roles in SSTFBs. Current collectors provide low-resistance electronic pathways to and from the electrode layers, while the substrate provides mechanical support and defines the surface on which the thin-film stack is built. From a manufacturing viewpoint, both also impose processing constraints. They must remain chemically stable and mechanically compatible with the deposition and post-treatment conditions used for the active layers. Noble metals and conductive metal foils such as Pt, Au, Al, and Cu are widely used in laboratory-scale SSTFBs because they provide stable interfaces and are compatible with vacuum processing (Ref 97, 98). Silicon wafers are also common because they offer smooth, defect-free surfaces and compatibility with microfabrication, but their cost, rigidity, and weight limit their relevance for large-area manufacturing (Ref 36, 99). Flexible metal foils and polymer substrates are increasingly being considered for lightweight and scalable SSTFB architectures. Their main implication is that the substrate becomes part of the processing constraint. Polymeric substrates limit the allowable temperature, whereas metal foils can affect the stack through surface roughness, oxidation, interdiffusion, or thermal expansion mismatch. Therefore, substrate selection influences layer adhesion, residual stress, interface quality, and the feasibility of post-deposition treatment.

Table 1 summarizes representative SSTFB material families for anodes, cathodes, solid electrolytes, and current collectors/substrates, highlighting their main electrochemical roles and key challenges.

Full-Stack Integration and Interface Control

Discussing SSTFB materials component-wise is useful for organizing the material requirements, but it does not give the full manufacturing picture. In an actual device, the electrodes, electrolyte and current collector layers have to be deposited and integrated in a specific sequence. A layer that appears suitable on its own may still become difficult to use if its deposition changes the surface, chemistry, or stress state of the layer beneath it. The interfaces between these layers need to be treated as functional regions of the cell, not only as boundaries between components. The electrolyte/anode and cathode/electrolyte interfaces must allow ion transfer while avoiding electronically leaky paths and resistive reaction layers (Ref 100, 101). These interface requirements apply to both Li- and Na-based SSTFBs, although the relevant interphase chemistry, metal/electrolyte wetting, and electrode/electrolyte compatibility depend on the specific alkali-ion system (Ref 102, 103). Current collector/electrode interfaces have a different requirement: they must provide electronic contact and adhesion without promoting oxidation, interdiffusion, or mechanical instability (Ref 104). These requirements are difficult to satisfy simultaneously because each interface is affected by the chemistry of the two neighbouring layers as well as by the thermal and mechanical history of the deposition process.

The main interface-related defects are summarized schematically in Fig. 2. The first group includes physical and microstructural discontinuities. Local voids or grain-boundary defects in the solid electrolyte, such as those shown for LLZO in Fig. 2(a) (Ref 105), can interrupt local ion transport and contribute to non-uniform current distribution near the interface. Poor physical contact is another common limitation, especially at solid cathode/solid electrolyte interfaces, where point contact or local gaps reduce the effective contact area available for ion transfer, as

Table 1 Summary of representative SSTFB material families and their key electrochemical roles, manufacturing constraints, and interface-related limitations

SSTFB Component	Representative material families	Functional relevance	Key challenges
Anodes	Alkali metal anodes, e.g., Li metal and Na metal	Very high capacity, low electrochemical potential	High reactivity; dendrite formation; unstable metal/electrolyte interface
	Si and Li-alloy anodes and Sn-/Sb-based Na-alloy anodes	High capacity; compatibility with thin-film and microfabrication routes	Large volume change; cracking; loss of contact; mechanical degradation during cycling
	Insertion/host-type anodes for Li- and Na-based systems, e.g., LTO, Ti-based oxides/phosphates, graphite, and hard carbon	Better structural stability; lower volume change during cycling	Lower capacity; alkali loss or phase changes during processing; thickness and interface control
Cathodes	Layered oxides, e.g., LCO, NMC, NCA, $NaMO_2$-type oxides	Established chemistries; high energy density	Alkali stoichiometry control; cation disorder or phase instability; crystallinity loss; post-annealing often required; electrode/electrolyte compatibility
	Spinels, e.g., LMO, LNMO	3D Li-ion diffusion; comparatively robust crystal structures	Phase purity; Mn volatility; oxygen non-stoichiometry; interface reactions
	Polyanionic cathodes	Good thermal and structural stability	Lower conductivity; thin-film integration challenges; possible post-treatment requirements
Solid electrolytes	LiPON	Benchmark thin-film electrolyte; stable against Li metal	Moderate ionic conductivity; strongly dependent on sputtering conditions; limited compatibility with high-temperature processing
	Oxide electrolytes, e.g., LLZO, LLTO and NASICON-type $Na_3Zr_2Si_2PO_{12}$ or β''-Al_2O_3-type electrolytes	Promising ionic conductivity and chemical stability	Densification challenges; alkali loss; grain-boundary resistance; secondary phase formation
	Sulphide electrolytes	Very high ionic conductivity	Moisture sensitivity; chemical reactivity; limited thermal stability; processing difficulty; possible formation of hazardous sulphur-containing species
	Polymer/composite electrolytes	Flexible and low-temperature processing	Lower room-temperature conductivity; mechanical and long-term stability limitations
Current collectors/substrates	Metals, e.g., Pt, Au, Cu, Al, stainless steel, SS	Good electrical conductivity and process compatibility	Cost for noble metals; oxidation; interdiffusion; thermal-expansion mismatch
	Si wafers/rigid substrates	Smooth surfaces; microfabrication compatibility	Cost; rigidity; thermal shock risk; limited relevance for large-area manufacturing
	Flexible substrates, e.g., metal foils or polymers	Scalability potential; lightweight and flexible architectures	Limited thermal tolerance for polymers; roughness; adhesion and process-compatibility issues

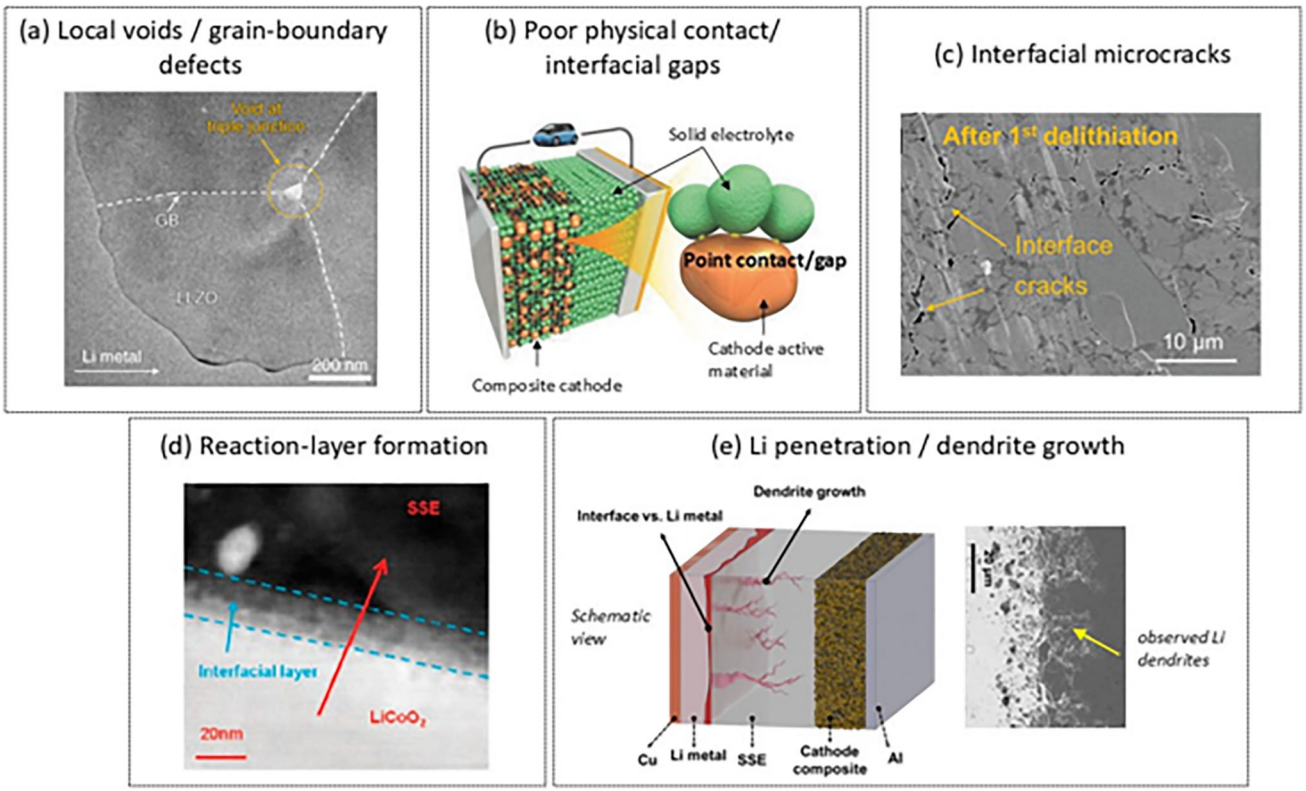

Fig. 2 Representative interface-related defects relevant to solid-state thin-film battery (SSTFB) integration: (a) local void formation at lithium lanthanum zirconium oxide (LLZO) grain-boundary/triple-junction regions. Reprinted with permission from X. Liu, R. Garcia-Mendez, A.R. Lupini, Y. Cheng, Z.D. Hood, F. Han, A. Sharafi, J.C. Idrobo, N.J. Dudney, and C. Wang, "Local electronic structure variation resulting in Li 'filament'formation within solid electrolytes," *Nature Materials*, 20(11), p 1485-1490, 2021, Springer Nature (Ref 105); (b) poor physical contact and interfacial gaps at the composite cathode/solid electrolyte interface. Reprinted with permission from L.-P. Wang, X.-D. Zhang, T.-S. Wang, Y.-X. Yin, J.-L. Shi, C.-R. Wang, and Y.-G. Guo, "Ameliorating the Interfacial Problems of Cathode and Solid-State Electrolytes by Interface Modification of Functional Polymers," *Advanced Energy Materials*, 8(24), p 1801528, 2018, John Wiley and Sons (Ref 106); (c) interfacial microcracks at the silicon/lithium phosphorus sulphide chloride (Si/LPSCl) composite interface after delithiation. Reprinted with permission from H. Huo, Y. Bai, S.L. Benz, T. Weintraut, S. Wang, A. Henss, D. Raabe, and J. Janek, "Decoupling the Effects of Interface Chemical Degradation and Mechanical Cracking in Solid-State Batteries with Silicon Electrode," *Advanced Materials*, 37(7), p 2415006, 2025, John Wiley and Sons (Ref 107); (d) reaction-layer formation at the lithium cobalt oxide ($LiCoO_2$)/solid electrolyte interface. Used with permission of IOP Publishing, from "Nanoscale interface modification of LiCoO2 by Al2O3 atomic layer deposition for solid-state Li batteries," J.H. Woo, J.E. Trevey, A.S. Cavanagh, Y.S. Choi, S.C. Kim, S.M. George, K.H. Oh, and S.-H. Lee, *Journal of The Electrochemical Society*, 159(7), 2012; permission conveyed through Copyright Clearance Center, Inc. (Ref 108); and (e) schematic (Reprinted from (Ref 109), available under CC BY 4.0 licenseat MDPI) and observed (Reprinted from (Ref 110), available underCC BY 4.0 license at Nature Communications) examples of lithium penetration/dendrite growth at the lithium-metal/solid electrolyte interface. These defects can reduce effective contact area, increase interfacial resistance, promote leakage or short-circuit pathways, and reduce cycling stability

illustrated in Fig. 2(b) (Ref 106). Cracks at or near the interface, shown in Fig. 2(c) (Ref 107), represent a related but more mechanically driven defect. They may form during processing, delithiation/lithiation, or thermal cycling and can lead to loss of contact or local separation between adjacent layers. Chemical and electrochemical degradation can create additional interface losses even when the layers appear physically continuous. Reaction-layer formation at electrode/electrolyte interfaces, as shown in Fig. 2(d) (Ref 108), can introduce resistive interphase regions and increase interfacial impedance during cycling or post-treatment. In cells using lithium metal, unstable interfaces can also promote lithium penetration and dendrite growth, as illustrated schematically and experimentally in Fig. 2(e) (schematic: (Ref 109), micrograph: (Ref 110)). This is an electrochemical failure pathway, but it is often assisted by local defects, current constriction, or weak interfacial regions. Since SSTFB layers are only a few micrometres thick, even localized interface damage can influence a large fraction of the active cell volume and strongly affect electrochemical performance and lifetime.

Several interface-engineering strategies have been used to reduce interfacial resistance, reaction-layer formation, and loss of contact in both Li- and Na-based SSTFBs. Thin buffer or interlayer coatings can be introduced to suppress

interdiffusion, improve adhesion, accommodate strain, or stabilize chemically reactive interfaces. Reported examples include ultrathin Al_2O_3 layers at LiPON/electrode interfaces (Ref 108, 111), surface-modified LiPON interfaces containing Li_2O/Li_3PO_4-type species (Ref 112, 113), and cathode-side interlayers such as $LiNbO_3$ or $BaTiO_3$ that can reduce resistive interphase formation or space-charge-related effects at oxide cathode/electrolyte boundaries (Ref 101). The deposition route also contributes to interface quality. Low-temperature or ion-assisted sputtering can help produce smoother LiPON-based films, while co-sputtering and related multicomponent deposition approaches provide a way to adjust interfacial chemistry and ionic transport properties (Ref 38, 114). For Na-based systems, related strategies include surface modification, artificial interphase formation, bilayer electrolyte architectures, and composite interlayers to improve Na/electrolyte contact and reduce interfacial resistance (Ref 115).

The broader point is that successful deposition of a single layer is not the same as successful stack integration. For SSTFB manufacturing, each processing step must preserve the layers that are already present, maintain acceptable roughness and defect levels, and avoid interfacial reactions that increase resistance or weaken adhesion. A route that is suitable for preparing an isolated anode, electrolyte, or cathode film may therefore still be unsuitable for full-cell fabrication if the subsequent layers cannot be added without damaging the existing structure. This is why manufacturing routes for SSTFBs must be assessed not only by the quality of individual layers, but also by their ability to produce chemically and mechanically stable interfaces throughout the complete device architecture.

Conventional Manufacturing Routes and Their Limitations

Vacuum-based methods remain central to SSTFB fabrication because they provide the level of film control needed for thin multilayer stacks. Sputtering is the most established route, particularly for LiPON electrolytes and oxide cathodes, where film uniformity and compatibility with sequential layer deposition are important (Ref 36, 116). PLD is useful for complex oxides and model studies as it can handle multicomponent targets and support controlled film growth, although lithium retention still requires careful process control (Ref 12, 116, 117). ALD is used differently from most line-of-sight physical vapour deposition routes. Because it provides conformal growth with precise thickness control, it is especially useful for ultrathin protective coatings, surface modification, and interface-engineering layers. These layers may not contribute much active material, but they can strongly influence interfacial reactions, contact stability, and transport across the stack. However, the low growth rate of ALD makes it less suitable for building thicker active electrode or electrolyte layers at practical rates (Ref 118). CVD and MBE are used more selectively, with CVD offering dense and conformal films and MBE serving mainly as a research tool for model interfaces and transport studies (Ref 20). The strong control that these methods offer over film quality comes at the cost of slow deposition, high equipment cost, and restricted deposition area, which imposes significant manufacturing-relevant restrictions. These limitations become more important when the target is not only a thin model layer, but a multilayer battery stack with enough active material to provide useful areal capacity. A further limitation, common to several vacuum-based routes, arises when Li or Na-containing materials are deposited. Depending on the process and any subsequent annealing step, metal loss, phase instability, and atmosphere-sensitive changes can make it difficult to preserve the intended composition and structure. Solution-based and printing methods address the scale and cost limitations of vacuum processing, but they do not remove the integration problem. Their advantage is that material can be deposited more flexibly, often over larger areas and with less reliance on high-vacuum infrastructure. The critical step there is what happens after deposition. The wet or particle-based layer must be converted into a functional solid film, and this conversion can alter both the microstructure of the layer and the chemistry of the interfaces.

In summary, a close analysis of conventional SSTFB fabrication approaches reveals that they enable either control or scale but a processing route that permits both continues to be elusive. For example, vacuum-based methods offer precise thin-film quality but pose considerable scale-up challenges, while solution and printing routes improve material placement and scalability but still require drying, densification, or heat treatment steps that can make final layer density and interface stability difficult to control. These trade-offs motivate the search for alternative manufacturing routes that can improve deposition rate and coating area while retaining sufficient control over composition, microstructure, and interfaces. Thermal spray processing is considered promising in this context and is deliberated in the following section, while the component-specific compatibility of SSTFB materials with thermal spray is discussed in "Thermal-Spray Compatibility Across SSTFB Components" section.

Thermal Spray as an Emerging Manufacturing Route for SSTFBs

Thermal spray is increasingly relevant to SSTFB manufacturing because it can potentially enable a transition from thin-film precision alone towards faster layer build-up and larger-area processing. Compared with many vacuum-based routes, it can provide higher deposition rates, larger-area coating capability, and greater flexibility in layer thickness and substrate geometry. Compared with slurry-based coating and printing routes, the deposited layer can be formed without organic binders, although post-treatment may still be required depending on the material and target microstructure. These differences make thermal spray relevant to consider for SSTFB manufacturing, but its usefulness depends on whether composition, microstructure, surface quality, and interfaces can be controlled at the level required for battery layers.

Different thermal spray processes access distinct combinations of particle temperature and velocity, as summarized in Fig. 3 (Ref 119). Plasma-based processes (such as atmospheric plasma spray (APS), suspension plasma spray (SPS), solution precursor plasma spray (SPPS)) operate at very high particle temperatures with moderate velocities, enabling complete melting and rapid solidification. While this is advantageous for depositing high-melting-point battery materials, it also increases the risk of volatilization in thermally sensitive compositions. In this context, it is pertinent to point out that the high thermal energy available in plasma spraying can be utilized for direct deposition of coatings from solution precursors, as it facilitates complete precursor decomposition and in-flight phase formation without the need for any pre-formed powder (Ref 120-122). At the same time, the final coating chemistry still depends on how the precursor evaporates, decomposes, and reacts during spraying, and whether the desired phase can be retained after deposition (Ref 123). Combustion-driven processes such as flame spray, high velocity oxy-fuel spray (HVOF), warm spray, and high velocity air fuel spray (HVAF) span regimes that progressively shift from thermally dominated to combined thermal-kinetic deposition as particle velocity increases and thermal energy decreases. In contrast, cold spray represents a purely kinetic energy-driven regime, in which particles remain in a solid state and bonding occurs through high-velocity impact and severe plastic deformation. Aerosol deposition (AD), although not

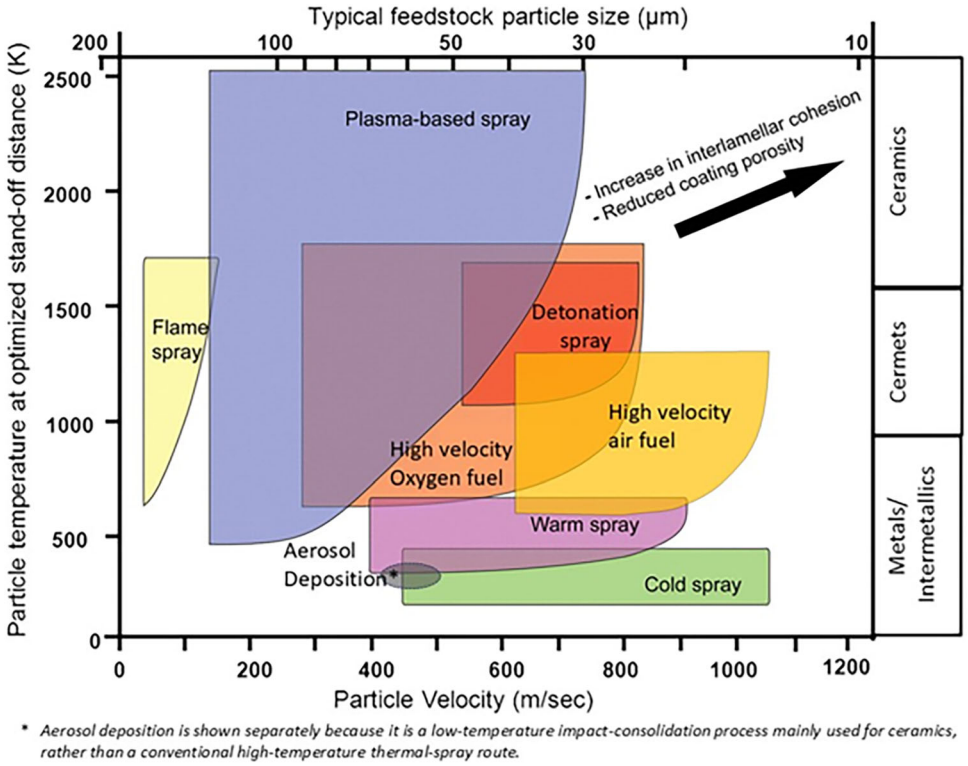

Fig. 3 Process map showing typical particle temperature–velocity ranges and feedstock particle sizes for major thermal spray variants. The map highlights the flexibility of thermal spray in processing different material classes by accessing a broad range of particle heat-up and acceleration conditions, which can be used to tailor coating microstructure and properties. Aerosol deposition is included as a related low-temperature impact-consolidation process and is marked separately because it is not a conventional high-temperature thermal-spray route. Adapted from A.S.M. Ang and C.C. Berndt, "A review of testing methods for thermal spray coatings," *International Materials Reviews* 59(4), p 179-223. Copyright © 2014 by Sage Publications. Reprinted by Permission of Sage Publications (Ref 119)

a conventional thermal-spray process, can also be included as a related low-temperature impact-consolidation route, where fine ceramic particles form dense layers through impact-induced fracture and consolidation rather than melting.

When thermal spray processes are applied to battery materials, the interaction between process physics and material chemistry, phase and microstructure, becomes the primary determinant of electrochemical functionality. Unlike most conventional coating applications such as those demanding wear and corrosion resistance, where full melting and dense splat formation are generally desirable, battery materials respond to thermal and kinetic exposure in more nuanced ways. The same spray conditions that degrade one battery component may be advantageous for another, particularly in the context of thin-film architectures.

In plasma-based processes, the high enthalpy of the plasma plume enables complete melting of the feedstock, and subsequent quenching upon impacting the substrate enables rapid solidification, facilitating the formation of finely structured coatings. For battery materials, this interaction can lead to multiple outcomes. While high temperatures and long residence times can promote alkali (Li/Na) volatilization or phase decomposition, or secondary phase formation in thermally sensitive compositions, such conditions support the deposition of dense ceramic electrolytes, and compositionally homogeneous multi-cation oxides (Ref 29, 124). Suspension and solution precursor routes further expand this processing capability by allowing submicron or liquid feedstocks, improved precursor mixing, and direct oxide formation from liquid precursors, which can support finer-scale coating architectures than are typically obtained using conventional powder-based approaches. As a result, plasma-based routes may be suitable for fabricating thin solid electrolytes and nanostructured electrodes, provided enthalpy and droplet/particle residence time are carefully controlled.

For highly phase-sensitive battery materials, the processing environment can be as important as the thermal input. Exposure to atmospheric oxygen, moisture, and high-temperature reactive species can accelerate lithium volatilization, alter oxygen stoichiometry, and promote formation of secondary phases in lithium-containing oxides and solid electrolytes (Ref 125). Consequently, alternative deposition approaches such as controlled-atmosphere thermal spraying and vacuum plasma spraying (VPS), where deposition occurs under inert or reduced-pressure environments, may offer advantages by reducing interactions with ambient gases and improving phase retention during deposition (Ref 126). Although these approaches generally involve greater equipment complexity and lower deposition throughput compared with conventional APS processes, they provide valuable alternative pathways for processing battery constituents whose electrochemical performance is highly sensitive to phase stability and environmental exposure during fabrication.

The previously mentioned high-velocity combustion processes such as HVOF and HVAF occupy a lower thermal energy-higher kinetic energy process–material interaction regime and are better suited for mitigating thermal degradation of feedstock relative to APS. The lower thermal energy exposure compared to plasma spraying reduces the risk of lithium evaporation and severe phase degradation, while still enabling partial or full melting of particles (Ref 127, 128). For battery electrodes, this can help preserve electrochemical phases while forming mechanically continuous coatings. However, it is to be noted that reduced extent of feedstock melting can limit densification, which is a critical requirement for solid electrolytes and separator-like layers. Consequently, these routes are often better suited for electrodes or interlayers than for fully dense electrolyte membranes, unless they are supplemented by post-deposition treatments.

Solid-state deposition routes, such as cold spray, introduce a fundamentally different process–material interaction. Since particles remain below their melting temperature, the feedstock stoichiometry, crystallinity, and oxidation state are largely preserved (Ref 129). This is particularly advantageous for metallic anodes, current collectors, and conductive interlayers where chemical fidelity is essential. At the same time, the reliance on plastic deformation for bonding restricts the direct deposition of brittle ceramic battery materials, which limits the applicability of cold spray for oxide electrodes or solid electrolytes. In this context, aerosol deposition (AD) has emerged as a solid-state route of interest for depositing ceramics. AD differs from conventional thermal-spray routes in that coating formation occurs mainly through impact-induced fracture, fragmentation, and consolidation of fine particles rather than through melting and splat solidification. Unlike cold spray of ductile metals, where particle plastic deformation plays a central role, AD is mainly relevant to ceramics despite its low processing temperature and is therefore indicated as such in Fig. 3. AD appears to be a promising route for fabricating dense ceramic battery layers while largely avoiding thermally induced phase degradation (Ref 130).

Across all thermal spray families, the end result is governed by the particle heat-up and acceleration resulting from the thermal and kinetic energy to which the injected feedstock is exposed to in-flight. These parameters determine whether a battery material is eventually deposited as a crystalline or amorphous, dense or porous, stoichiometric or compositionally shifted layer. Each of these states may be either beneficial or detrimental depending on the

targeted battery component. Thermal spray should, therefore, be viewed as a flexible processing toolbox, where different spray variants permit distinct processing environments that can be aligned with the requirements of each SSTFB layer, as will be discussed in the following section.

Thermal-Spray Compatibility Across SSTFB Components

The previous sections outlined the material requirements for SSTFB components along with some material families of interest and the process conditions associated with different thermal spray routes. This section attempts to connect the above two. The primary focus is on whether the different materials of interest can yield the required crystallographic, chemical and microstructural attributes after thermal spray processing to be interesting from the standpoint of functionality sought in SSTFBs. This distinction is necessary because spray conditions suitable for one battery component may not be transferable to another, as each material class responds differently to heat input, particle impact, oxidation, and post-deposition cooling. A process that helps form a dense ceramic layer may be too aggressive for a lithium-rich or phase-sensitive compound. Similarly, a lower-temperature route may preserve chemistry better, but may not provide enough particle deformation or densification while spraying some types of materials. Component-wise candidate SSTFB material–process compatibility is therefore discussed here in terms of feedstock response, phase and composition retention, coating formation, and integration within the SSTFB stack.

Anode

From a thermal-spray manufacturing perspective, anode materials differ strongly in their processability. Metallic alkali anodes, especially lithium and sodium, which are electrochemically attractive because of their high theoretical capacity and low electrochemical potential, are poorly suited for conventional thermal-spray deposition. Their low melting point, high chemical reactivity, and sensitivity to oxidation and evaporation make it difficult to process them under high-temperature spray conditions (Ref 30, 131). For predominantly thermally sprayed SSTFB architectures, lithium metal is therefore more appropriate to be introduced by a separate low-temperature or vacuum-based step rather than deposited directly by thermal spray. Alternatively, an anode-free configuration may be used, in which no active anode is deposited during fabrication and lithium is plated onto the anode-side current collector during the first charge (Ref 132).

Silicon and lithium-alloy anodes may be more compatible with thermal spray processing than metallic lithium, but they are not straightforward thermal-spray candidates either. Rapid heating and cooling during deposition can lead to feedstock oxidation, introduce residual stresses, or alter the microstructure in ways that adversely affect electrochemical performance (Ref 133, 134). For Si-based anodes, the intrinsic volume change during cycling remains relevant in the context of thermal-spray processing, because a sprayed anode layer would need to maintain mechanical integrity and electrical contact during repeated lithiation and delithiation.

Oxide-based insertion anodes, such as LTO, appear more compatible with thermal-spray processing because of their relatively small volume change during cycling and better thermal stability (Ref 31). LTO is thus a useful model system for studying how lithium-containing anode materials respond to plasma or suspension spray conditions. However, even for LTO, lithium volatilization, secondary phase formation, and stoichiometry preservation remain important issues when the material is exposed to high-temperature spray conditions (Ref 124, 135).

For SSTFBs, anode compatibility also depends on the full stack architecture. The anode layer must integrate with the adjacent electrolyte and current collector, while maintaining controlled thickness, adhesion, and interface stability. This is especially important for rigid substrates such as silicon wafers and glass, as well as for metal foils used in more scalable architectures (Ref 36). When these stack-level requirements are combined with the thermal and kinetic conditions of spray deposition, the acceptable process window becomes relatively narrow. Heat input and residence time influence alkali retention and oxidation, while substrate temperature and impact conditions affect stress build-up, adhesion, and interfacial degradation (Ref 136). In this context, lower-enthalpy or solid-state deposition routes appear more suitable for metallic anodes and conductive interlayers, while plasma or suspension-based routes are more relevant for oxide insertion anodes such as LTO.

Cathode

From a thermal-spray manufacturing perspective, cathode materials are challenging because many of the promising candidates contain lithium/sodium and have complex crystal structures that are sensitive to high-temperature processing (Ref 30). Layered oxide cathodes such as $LiCoO_2$ (LCO), $LiNi_xMn_yCo_zO_2$ (NMC), and $LiNi_{1-x-y-}Co_xAl_yO_2$ (NCA) are widely used in conventional thin-film and bulk battery systems, but their layered structures can be disturbed during spraying if lithium is lost, oxygen stoichiometry changes, or cation disorder develops, leading

to formation of electrochemically inactive secondary phases during thermal spraying (Ref 31). For this reason, layered cathodes may require lithium-rich feedstocks, lower-enthalpy spray conditions, or post-deposition annealing to retain or recover the desired structure. Similar concerns would apply to layered $NaMO_2$-type cathodes in sodium-based systems, where sodium retention, oxygen stoichiometry, cation ordering, and phase stability would need to be preserved during deposition and any post-treatment. However, these materials should be regarded as candidates requiring spray-specific validation rather than established thermal-spray SSTFB cathodes.

Spinel-type cathodes such as $LiMn_2O_4$ (LMO) and $LiNi_{0.5}Mn_{1.5}O_4$ (LNMO) may offer somewhat better compatibility with thermal spray because of their more robust three-dimensional crystal structures (Ref 137, 138). However, depending on the spray conditions, the final layer may still undergo compositional changes, such as oxygen imbalance or manganese loss, along with structural changes at the surface or through secondary phase formation. Therefore, their compatibility should be assessed under process-specific conditions rather than assumed from their bulk thermal stability.

Polyanionic materials, especially $LiFePO_4$ (LFP), and related Na-based polyanionic cathodes, have comparatively good structural resilience and thermal stability owing to their phosphate-based olivine structure. Even so, severe heat exposure can lead to phosphate-group degradation, alkali loss, or changes in crystallinity (Ref 139, 140). As with layered and spinel cathodes, the final electrochemical response depends on how well composition, phase structure, and microstructure are retained or restored after thermal spray deposition.

Recent work on thermally sprayed cathode materials shows that particle temperature, plasma enthalpy, spray atmosphere, and substrate temperature must be carefully controlled to limit compositional changes and preserve electrochemical activity (Ref 31). In many cases, post-deposition annealing or related thermal treatments are needed to restore crystallinity and recover the required electrochemical properties (Ref 30). This does not rule out thermal spray for cathodes, but it shows that process design must balance chemistry retention during deposition with the crystallinity and microstructure needed after deposition or post-treatment. Hence, for cathodes, plasma-based routes are more relevant when melting, crystallization, or oxide formation is required, whereas lower-enthalpy combustion or controlled-atmosphere approaches may be preferable for alkali-rich and phase-sensitive compositions.

Electrolyte

For electrolytes, thermal spray compatibility is especially difficult to assess because a dense-looking coating need not necessarily be a functional electrolyte. The sprayed layer must retain the phase, stoichiometry, and defect structure needed for ionic transport, while avoiding electronic leakage paths through pores, cracks, or connected splat boundaries (Ref 29, 31, 141). For this reason, successful deposition of an electrolyte coating should be followed by careful characterization and benchmarking against conventionally deposited SSTFB electrolytes, to tune the spray process towards the required electrolyte properties.

LiPON remains the benchmark electrolyte in conventional SSTFBs, but thermal spraying is not an obvious route for its processing. For example, in conventional vacuum-based approaches like sputtering, its amorphous structure and nitrogen-containing phosphate network are known to be strongly controlled by sputtering conditions and film composition; these features would be difficult to preserve under high-temperature spray conditions (Ref 82). LiPON is therefore more useful as a performance reference for thin-film electrolytes than as a likely direct thermal-spray feedstock.

The oxide-based electrolytes such as LLZO and LLTO are more relevant to thermal spray because they can tolerate higher processing temperatures than LiPON or sulphide electrolytes (Ref 31, 141, 142). Recent studies have shown that LLZO and LLZTO ($Li_{6.5}La_3Zr_{1.5}Ta_{0.5}O_{12}$) coatings can be deposited by APS and SPS. However, lithium loss, secondary phase formation, surface roughness, and reduced ionic conductivity remain important limitations (Ref 31, 141). While LLTO offers good oxide stability, in thin-film or coating forms it may suffer from microstructural heterogeneity and grain-boundary resistance, which can reduce total ionic conductivity after high-temperature processing (Ref 143).

Sodium-based oxide electrolytes provide a related but chemically distinct case. NASICON-type Na-ion conductors such as $Na_3Zr_2Si_2PO_{12}$, together with β''-Al_2O_3-type electrolytes, are relevant ceramic electrolyte families for Na-based solid-state systems. From a thermal-spray perspective, NASICON-type oxides are particularly important because plasma-sprayed $Na_3Zr_2Si_2PO_{12}$ has been reported as a dense Na-superionic conductor, indicating that spray processing can be extended to selected Na-ion ceramic electrolyte chemistries (Ref 144). However, this should be interpreted as electrolyte-level processability evidence rather than proof of a complete Na-based SSTFB architecture. (Ref 8, 87).

Li/Na-based sulphide electrolytes are poorly suited to conventional thermal-spray methods. Their moisture sensitivity and chemical reactivity already complicate thin-

film processing, and high-temperature or open-atmosphere spraying adds further safety and phase-stability concerns, including the possible formation of volatile sulphur-containing species such as H_2S (Ref 92, 145).

Overall, thermal spraying of candidate SSTFB electrolytes requires careful control of spray parameters, feedstock characteristics, and post-deposition thermal treatment to preserve phase purity and ionic transport properties. Feedstock chemistry and spray atmosphere control phase retention, while thermal exposure and substrate conditions determine whether dense coatings can be obtained without losing alkali content or accumulating damaging defects. The eventual target from a functional standpoint is not just a dense coating, but an electronically insulating, ionically conductive, chemically stable layer with limited defect pathways and acceptable interfacial resistance. For oxide electrolytes, APS and SPS can be interesting thermal spray routes because they can provide the thermal input needed for ceramic coating formation. However, controlled-atmosphere or post-treatment-assisted approaches may be needed where alkali retention and phase purity are critical.

Current Collector and Substrate

As introduced in "Current Collectors and Substrates" section, current collectors and substrates have related but distinct roles in SSTFBs. In the thermal-spray context, metallic current collectors and conductive interlayers are realistic near-term deposition targets, whereas substrates such as Si wafers, glass, metal foils, or polymers mainly define the allowable heat input, particle impact conditions, roughness, and post-treatment window. Compared with alkali-containing ceramics, metallic layers are generally more tolerant to particle impact, high local heat flux, and thermal stresses during thermal spray coating deposition (Ref 146). Materials such as stainless steel, aluminium, titanium, copper, and nickel-based alloys also provide the electrical conductivity and mechanical robustness needed for current collectors or conductive interlayers. This makes them more immediately compatible with thermal spray than phase-sensitive cathodes or solid electrolytes (Ref 29, 31).

Noble-metal current collectors such as Pt and Au are widely used in laboratory-scale SSTFBs because of their chemical stability and compatibility with vacuum processing. However, their high cost limits their translation for large-scale thermal-spray manufacturing (Ref 147, 148). Silicon wafers are also common in thin-film battery research, but they present a different limitation: they are less suitable for direct thermal-spray processing because they can be susceptible to thermal shock and fracture during high-temperature or high-impact deposition (Ref 149, 150).

Metal foils and sheets are more attractive substrates for thermally sprayed battery designs because they can tolerate mechanical and thermal loads better (Ref 151, 152). They are also more compatible with scalable processing concepts than rigid silicon wafers. However, their use is not without constraints. The surface condition of the foil can affect adhesion, while oxide formation, interdiffusion, and thermal-expansion mismatch can influence the stability of the interfaces, especially when several layers are deposited sequentially.

Flexible polymer substrates are more difficult to combine with conventional thermal spray. Most of these processes involve local thermal exposure above the stability limits of common polymers such as PET and polyimide (Ref 153). Deposition on polymeric substrates would therefore require low-temperature spray variants, buffer layers, active cooling, or indirect deposition strategies (Ref 154).

In summary, for practical SSTFB manufacturing, substrate selection must be considered together with the intended stack architecture, any post-deposition treatment, and the need to maintain interfacial stability. Metallic current collectors and interlayers are more compatible with lower-temperature or kinetic routes such as cold spray, warm spray, HVAF, or HVOF, where oxidation and substrate overheating can be better limited.

The suitability of different thermal spray processes for SSTFB components is summarized in Fig. 4. The compatibility map shows how increasing thermal exposure can expand access to dense ceramic electrodes and electrolytes, but also increases the risk of alkali loss and phase changes. Lower-temperature, high kinetic energy routes are more favourable for metallic layers and chemically sensitive constituents, although they may not provide sufficient densification for electrolyte layers. At the same time, it is pertinent to note that the higher temperature routes have also been implemented to deposit metallic layers via careful control of spray parameters and are accordingly indicated in the figure (Ref 155, 156). This comparison highlights an important point for future SSTFB development: thermal spray should first be evaluated against the requirements of established SSTFB materials and architectures. For the specific spray routes that prove useful for selected layers, later development may involve adapting feedstock chemistry, layer architecture, or post-treatment conditions to improve alkali retention, phase stability, thermal robustness, and tolerance to rapid solidification. This materials-design perspective is further discussed in the Outlook section.

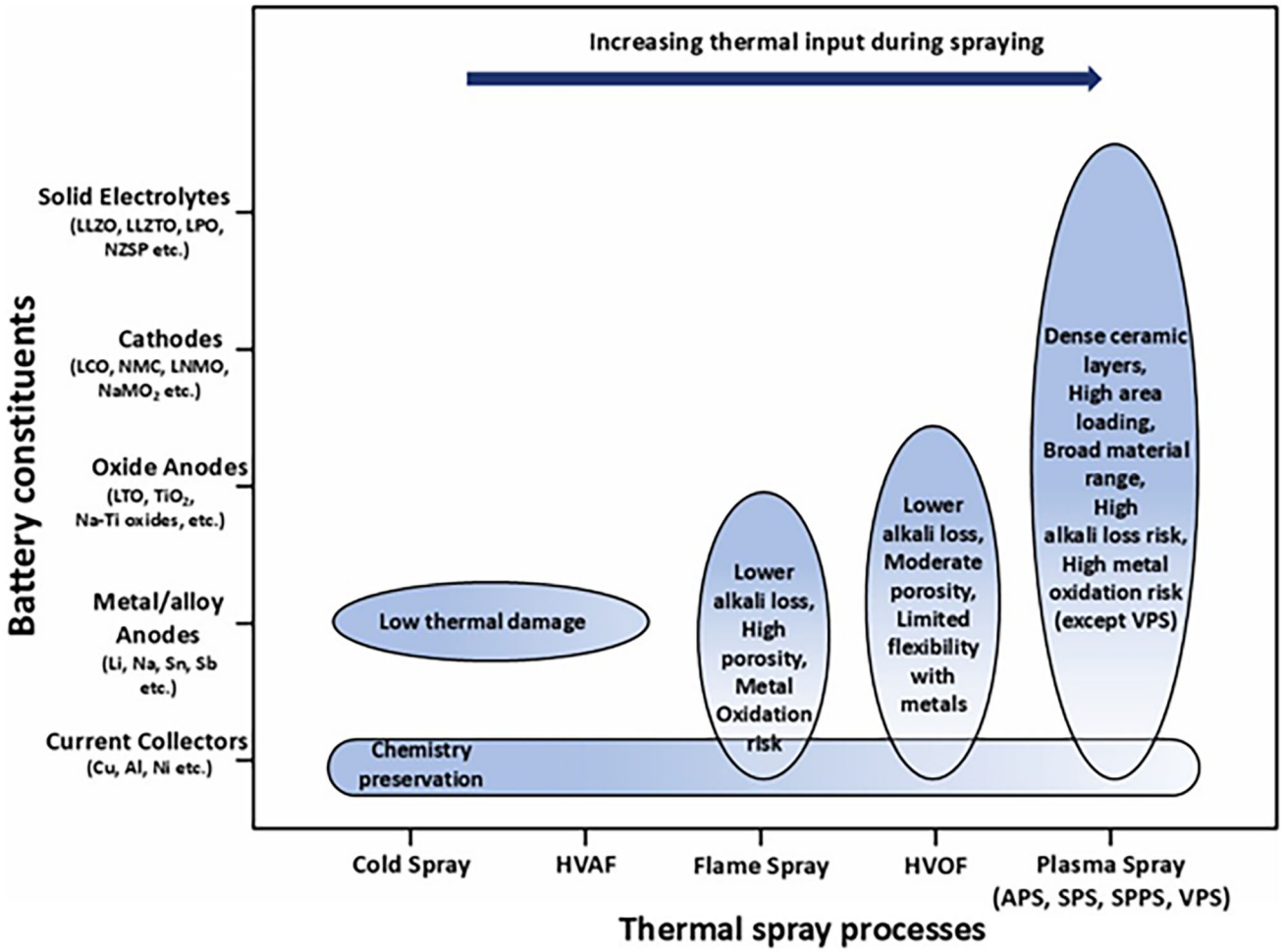

Fig. 4 Schematic summary of the relative compatibility between thermal-spray process families and candidate materials for SSTFB components. The map highlights the trade-off between chemistry/phase preservation at lower thermal input and dense ceramic-layer formation at higher thermal input

Current Status of Thermal-Spray-Based SSTFB Research

Thermal spray has been used for battery-material synthesis for several years, before its more recent consideration as a direct coating and film fabrication route. Flame spray pyrolysis (FSP) and plasma-based processes can produce nanoscale lithium and transition-metal oxides directly from precursor solutions or aerosols. These approaches have been used to synthesize $LiFePO_4$ (Ref 157), Li_2MSiO_4 (M = Fe, Mn), NMC-type cathodes, and multi-cation oxides with tunable particle size and crystallinity (Ref 158-160). Plasma-based synthesis routes, including thermal plasma pyrolysis and plasma spray-assisted precursor decomposition, have also enabled the production of high-purity and compositionally uniform powders of cathode-relevant materials such as NMC and $LiNi_{0.8}Co_{0.15}Al_{0.05}O_2$ (Ref 158, 159). This powder-synthesis work is relevant because it shows that flame and plasma environments can control morphology, phase formation, and defect chemistry. However, direct fabrication of functional SSTFB layers is a more demanding problem because the deposited coating must also satisfy thickness, roughness, interface, and electrochemical requirements.

To date, thermal spray has been explored at different levels of device complexity, from single battery layers to bilayer configurations and early multilayer stacks. Single-layer studies mainly show whether a material can be deposited and remains electrochemically active. Bilayer and interface studies start to test contact quality, charge-transfer behaviour, and compatibility between adjacent layers. Realization of multi-layer or full-stack configurations is more demanding because they introduce stack-level challenges that are not encountered in single-layer coatings. Interfaces formed during sequential deposition become buried as additional layers are added, making their contact quality and chemical stability difficult to correct later. Roughness from an underlying layer can also be

transferred to subsequent layers, reducing effective contact area and promoting local gaps or non-uniform current distribution. Repeated thermal exposure and residual stress can further influence ionic transport across electrolyte/electrode interfaces and electronic transport through the electrodes and current collectors. Accordingly, the following sections discuss the current status of thermal-spray-based SSTFB demonstrations by increasing architectural complexity.

Single-Layer Demonstrations

Single-layer studies form the foundation of thermal-spray-based SSTFB development because they isolate the response of one material to the spray process before the added complexity of a full stack is introduced. At this level, the main purpose is to establish whether the intended phase can be retained or recovered, whether secondary phases form, and whether the sprayed layer shows measurable electrochemical activity. It is an important first step, but it should not be read as direct evidence of device-level performance. Among anode materials, $Li_4Ti_5O_{12}$ (LTO) has been the most widely explored by thermal spray because of its broader appeal as a stable oxide anode. This is owing to its zero-strain spinel structure, which limits volume-change-related degradation during cycling. Early studies employing APS of LTO produced coatings showing electrochemical activity near $\sim$ 1.55 V vs. Li/Li^+, but x-ray diffraction (XRD) and Raman analyses also showed the presence of substantial TiO_2 and sub-stoichiometric titanate phases (Ref 161). This showed both the promise and the limitation of spraying LTO: the material can remain electrochemically active, but lithium loss and phase decomposition are difficult to avoid. Later work using SPS improved phase retention by enabling finer feedstock injection. Mathiyalagan et al. (Ref 124) obtained coatings with approximately 76 wt.% spinel LTO and stable cycling behaviour. Hasani et al. (Ref 29) used synchrotron μXRD and micro-x-ray fluorescence (μXRF) to show that even when the spinel phase remained dominant overall, local lithium depletion near the substrate could form $Li_2Ti_3O_7$, Li_2TiO_3, and TiO_2.

APS has also been used to fabricate amorphous LTO coatings. Wu et al. (Ref 162) reported that rapid splat quenching inhibited spinel formation. The as-sprayed amorphous films showed smoother Li-ion diffusion and lower interfacial impedance than crystalline LTO, giving better initial capacity retention. However, during extended cycling, partial recrystallization, interfacial reactions, and microcracking were observed. This indicates that amorphous LTO can be useful initially, but the amorphous-to-crystalline transition can influence long-term stability. In another work, Yost et al. (Ref 135) deposited dual-oxide TiO_2/LTO coatings by APS as binder-free, all-active-material electrodes. By adjusting plasma energy, they tuned the TiO_2/LTO ratio and the corresponding capacity, showing that plasma-spray parameters can directly influence electrochemical response through chemistry control.

Recent comparative investigations have further clarified the influence of thermal spray processing conditions on the structural and electrochemical behaviour of LTO thin-film anodes (Fig. 5a, b, c, and d) (Ref 163). By systematically comparing APS, SPS, and HVOF sprayed coatings using synchrotron μXRD/μXRF (Fig. 5d), XPS (Fig. 5e, f, and g), and electrochemical characterization, it was demonstrated that the thermal history associated with each process governs lithium retention, phase stability, and ultimately electrode performance. HVOF and APS retained a larger fraction of the spinel $Li_4Ti_5O_{12}$ phase, whereas SPS exhibited greater formation of Li_2TiO_3 and TiO_2 due to increased lithium loss and thermal decomposition. Interestingly, despite the higher phase retention achieved by HVOF, APS coatings exhibited the most favourable electrochemical response, highlighting that electrochemical performance depends not only on phase constitution but also on coating microstructure.

Research into thermal sprayed single-layer cathodes shows a similar balance between deposition feasibility and phase stability. LCO has been the most intensively studied cathode material. APS has been shown to deposit LCO films greater than 5 μm thick, with areal capacities exceeding 5 mAh cm^{-2} after post-annealing at 520 °C for 2 h (Ref 164). This is nearly an order of magnitude higher than typical sputtered films and demonstrates one of the main advantages of thermal spray: rapid active-layer build-up. At the same time, the need for post-annealing shows that the layered R3m structure is at least partly degraded during spraying and must be restored before useful electrochemical performance is obtained. Although direct thermal-spray demonstrations of LNMO for SSTFBs remain limited, spinel cathodes are relevant to consider because they may tolerate lower-enthalpy spray routes better than more phase-sensitive layered oxides.

Evidence from other thermally sprayed multicomponent oxides also shows that volatility and phase purity remain important processing constraints. For example, studies on HVOF-sprayed $La_{0.8}Sr_{0.2}Ga_{0.8}Mg_{0.2}O_3$ electrolytes for solid oxide fuel cells show that stoichiometry and phase formation must still be controlled during lower-enthalpy spraying (Ref 165). This processing analogy suggests that lower-enthalpy flame-spray routes may be worth evaluating for complex cathode chemistries such as LNMO for SSTFBs. Nonetheless, for layered and spinel cathodes, lithium evaporation, structural disorder, and secondary phase formation remain major limitations. Post-spray

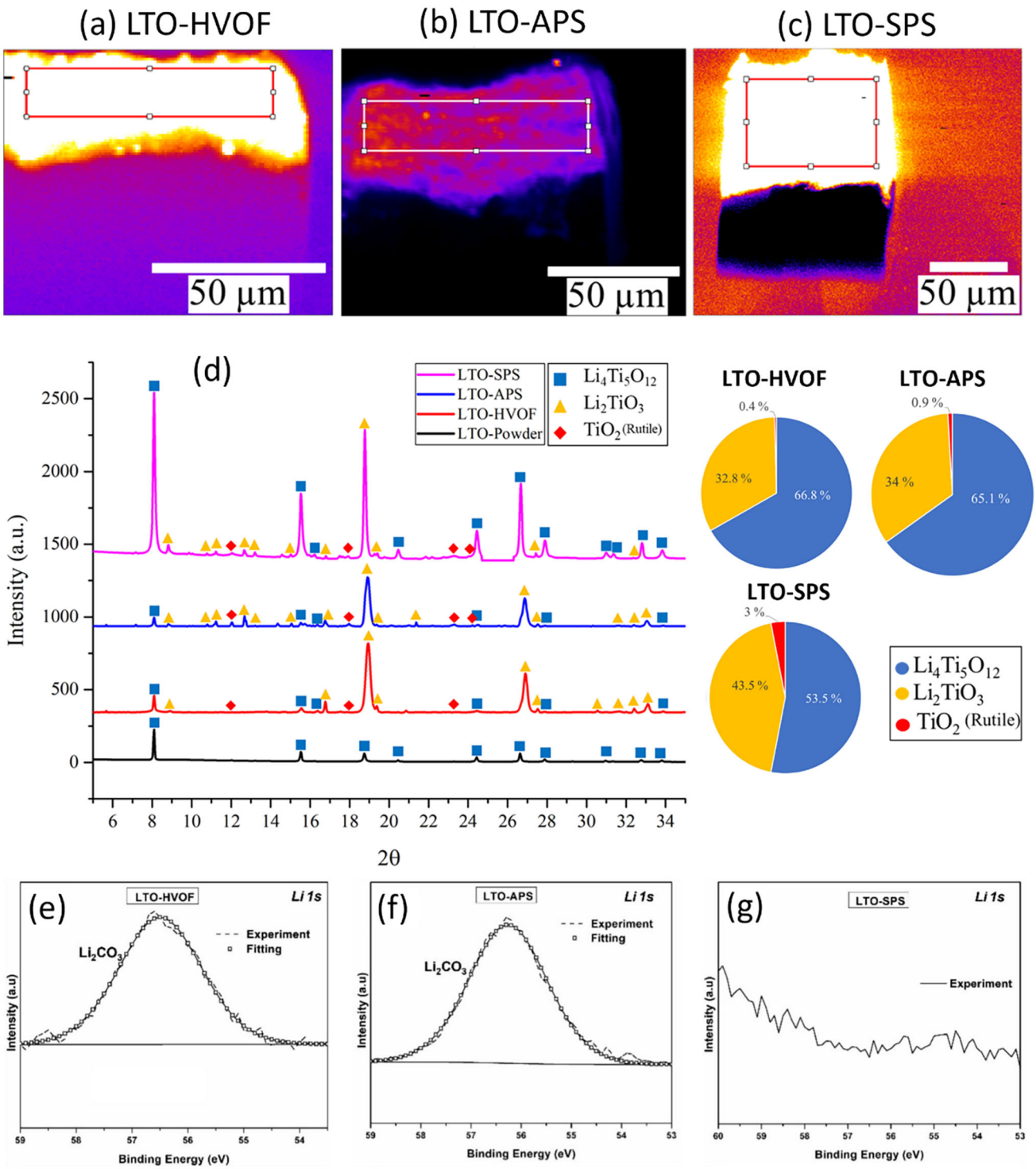

Fig. 5 Synchrotron µXRD analysis of thermally sprayed LTO thin-films: (a-c) mapped Regions of Interest (ROIs); (d) representative integrated patterns and their Rietveld-derived phase fractions shown in pie charts; XPS spectra of Li 1 s in LTO thin-films produced by (e) HVOF, (f) APS, and (g) SPS showing the state and retention of Li in the thermal-sprayed LTO anode. Reprinted from (Ref 163), available under CC BY 4.0 license at ScienceDirect

annealing or loss-compensation via use of lithium-rich feedstock strategies may therefore be needed.

Solid electrolytes have received particular attention because they are central to SSTFB operation. LLZTO coatings deposited using a variety of suspension plasma

spray (SPS) parameters achieved thicknesses of 15-30 µm. This study showed that suspension stability and spray parameters strongly affect phase retention, crystallinity, cracking, and Li-ion conductivity (Ref 166). The reported as-sprayed SPS coatings retained a high fraction of the cubic LLZTO phase, showed crystallinity close to 75%, and retained most of the Li content of the starting powder. The highest reported room-temperature ionic conductivity was of the order of 10^{-8} S cm^{-1}. This suggests that SPS can produce ionically conductive garnet-type coatings, but the conductivity remains well below that of dense bulk garnet electrolytes. Phase retention, lithium loss, secondary phase formation, cracking, and suspension/process optimization remain key issues.

APS has been explored separately for larger-area LLZO electrolyte films, resulting in thicknesses from 30 to 300 µm, including A4-size coatings, and freestanding electrolyte films were obtained after removal from the metallic substrate (Ref 141). In this case, post-annealing was a central part of the fabrication methodology. Annealing the APS coating at 1050 °C for 10 h was identified as the most suitable condition, giving a room-temperature ionic conductivity of 3.82×10^{-5} S cm^{-1}. The 300 µm-thick films also showed a flexural strength of about 157 MPa. Li/LLZO/Li and Li/LLZO/$LiFePO_4$ cells assembled using these films showed stable cycling, although interfacial contact remained a limiting factor. This study supports the scalability of garnet electrolyte processing, but also shows that post-treatment and interface management are essential for useful electrolyte performance.

Sun et al. (Ref 167) fabricated dense γ-Li_3PO_4 (LPO) solid-electrolyte coatings by APS, with nearly full densification ($< 1\%$ porosity) and ionic conductivity up to 4.6×10^{-8} S cm^{-1}. The coatings retained the γ-phase, a high-temperature polymorph with favourable Li^+ mobility, and showed columnar grains with chemical inter-splat bonding. Slight lithium enrichment, with Li/P ratios of 3.02-3.17 compared with the nominal value of 3, was attributed to preferential phosphorus loss from molten droplets during spraying. The Li/P ratio increased for smaller feedstock particles and longer spray distances, consistent with greater in-flight evaporation loss. This slightly Li-rich composition may have generated interstitial Li^+ defects that enhanced ionic transport. This work is important because it showed that plasma spraying can produce functionally conductive oxide electrolyte coatings without post-annealing in some systems, although the conductivity is still modest compared with the best electrolyte benchmarks.

Representative electrochemical responses from thermally sprayed LTO, LCO, and LPO layers are shown in Fig. 6, which should be read together with the test configuration used in each study. In the APS-LTO work shown in Fig. 6(a), the sprayed LTO layer was deposited on Cu mesh and tested as an electrode in a conventional Li half-cell, with Li metal as the counter electrode and $LiPF_6$-containing liquid as the electrolyte (Ref 161). In the APS-LCO work shown in Fig. 6(b), the sprayed LCO cathode was post-annealed and then assembled with a gel polymer electrolyte (GPE) and Li metal foil in a coin-type LCO/GPE/Li cell (Ref 164). In the APS-LPO work shown in Fig. 6(c), the free-standing electrolyte deposits were measured by electrochemical impedance spectroscopy (EIS) using Ag electrodes on both sides of the coating, rather than as a complete battery cell (Ref 167). These examples show that sprayed battery constituents can exhibit measurable electrochemical functionality in the reported test configurations, although the response remains closely linked to phase retention, microstructure, and post-deposition treatment.

Beyond the Li-based examples discussed above, there is also one relevant Na-based example for NASICON-type $Na_3Zr_2Si_2PO_{12}$ (NZSP) electrolyte layers. Bu et al. used plasma spraying to deposit NZSP layers for all-solid-state sodium-ion batteries, using different spray conditions and powder particle sizes (Ref 144). This study is useful for the present discussion as it shows both the potential and the difficulty of spraying a Na-containing electrolyte. Dense APS NZSP layers could be obtained, with an apparent porosity below 3%, which the authors attributed to the relatively low melting point of NZSP. However, the deposits also showed preferential evaporation of Na and P during spraying, leading to a large deviation from the starting powder composition. The powder particle size was identified as an important factor controlling this evaporation loss. After annealing, the electrolyte conductivity increased, reaching 1.93×10^{-4} S cm^{-1} at 200 °C for the sample annealed at 1000 °C. While this provides useful processability evidence for Na-based electrolyte layers, it also shows that alkali retention and composition control remain important issues. For Na-containing cathodes and anodes, the available thermal-spray evidence is still much more limited.

Thermal-sprayed metallic single layers are relevant mainly as analogues for anodes, interlayers, and current collectors. Cold-sprayed Zn has been explored for aqueous Zn-ion batteries, producing deposits with high areal loading, strong adhesion, and binder-free architectures. Unlike high-temperature plasma processes, cold spray can preserve metallic Zn without oxidation, making it attractive for large-area Zn electrodes (Ref 168, 169). These examples are useful for understanding metallic-layer processing, but they should be framed carefully because they are not all direct SSTFB demonstrations.

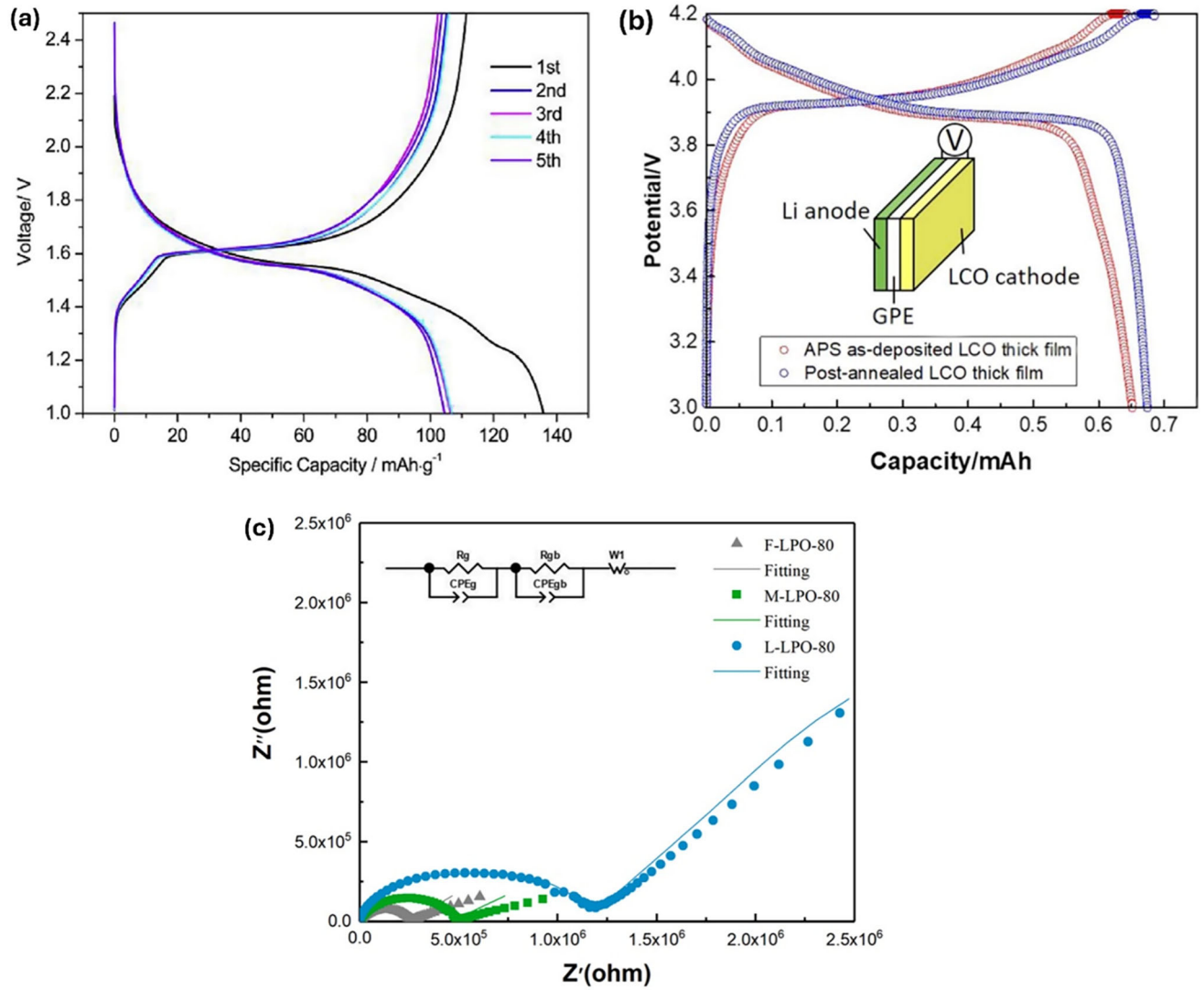

Fig. 6 Electrochemical performance of representative thermally sprayed battery constituents after incorporation into their reported test configurations: (a) charge–discharge cycles of an APS-sprayed $Li_4Ti_5O_{12}$ (LTO) anode deposited on Cu mesh and tested in a Li half-cell with Li metal counter electrode and $LiPF_6$-containing liquid electrolyte, showing reversible lithiation behaviour. Reprinted from *Ceramics International*, 45(17), X. Liang, Y. Wang, X. Zhang, D. Han, L. Lan, and Y. Zhang, "Performance study of a Li4Ti5O12 electrode for lithium batteries prepared by atmospheric plasma spraying," p 23750-23755, Copyright (2019), with permission from Elsevier (Ref 161); (b) charge–discharge curves of an APS-sprayed $LiCoO_2$ (LCO) cathode tested in a coin-type LCO/gel polymer electrolyte (GPE)/Li cell after post-annealing, showing recovery of electrode activity Reprinted from (Ref 164), available under CC BY 4.0 license at IOPScience; and (c) Nyquist plot of APS-deposited Li_3PO_4 (LPO) solid electrolyte measured by EIS using Ag electrodes on both sides of a free-standing electrolyte deposit, showing the effect of feedstock particle size on the impedance response. Reprinted from *European Ceramic Society*, 42(10), Y.-Q. Sun, X.-T. Luo, Y.-S. Zhu, X.-J. Liao, and C.-J. Li, "Li3PO4 electrolyte of high conductivity for all-solid-state lithium battery prepared by plasma spray," p 4239-4247, Copyright (2022), with permission from Elsevier (Ref 167). These examples demonstrate that thermally sprayed electrodes and electrolytes can show electrochemical functionality, while also highlighting the importance of phase control, microstructure, test configuration, and post-treatment

Overall, single-layer studies show that thermal spray can produce electrochemically active battery-relevant coatings. Their main value is as evidence of thermal spray process–SSTFB material compatibility rather than full device validation. They also show the main recurring issues: lithium/sodium volatility, secondary phase formation, local stoichiometry changes, residual porosity, and the need for post-treatment.

Interface-Focussed Demonstrations

After single-layer validation, the next level is to examine how thermally sprayed battery layers interact with neighbouring layers and interfaces. In the previous section, sprayed electrodes or electrolytes tested in conventional electrochemical configurations were discussed as single-layer demonstrations when the sprayed layer itself is the

main subject of the study. The present section instead focuses on studies where interface quality, roughness transfer, contact formation, or compatibility between adjacent battery constituents is the main focus. These studies are more informative than isolated layer tests because they begin to capture the buried-interface issues that are central to SSTFB operation. Compared with single-layer coating studies, far fewer thermal-spray studies have examined interface-focussed configurations or buried interfaces relevant to SSTFB stacks. The available examples are therefore best viewed as early indicators of integration challenges rather than as mature device demonstrations.

One representative example is the laser post-processing of APS single-layer LTO (Fig. 7a, b, c, and d), single-layer LLZO (Fig. 7e, f, g, and h), and the LTO–LLZO bilayer architecture (Fig. 7i, j, k, and l) to improve the surface quality of thermally sprayed battery components (Ref 170). Laser treatment effectively reduced the surface roughness and modified the near-surface microstructure without altering the crystalline phases or chemical state of LLZO, highlighting the potential of laser surface engineering as a post-processing strategy for thermal-sprayed battery materials.

The study further demonstrated that individual battery constituents exhibit distinctly different responses to laser irradiation owing to differences in their melting behaviour, optical absorption, and heat-transfer characteristics. This finding is particularly important for multilayer battery fabrication, where the surface topography of one deposited layer is inevitably transferred to subsequent layers, thereby influencing the overall interface quality and cell performance. As evident from the cross-sectional micrographs, laser treatment of the single-layer coatings resulted in controlled material removal and a significant reduction in surface roughness. However, when the optimized laser parameters established for the single-layer LLZO coating (Fig. 7f and h) were directly applied to the LTO–LLZO bilayer structure (Fig. 7j and l), complete ablation of both layers occurred. These observations highlight the complex interactions between the laser and multilayer architectures, demonstrating that laser processing parameters optimized for individual layers cannot be directly translated to multilayer systems. Instead, the thermal response is strongly governed by the combined material properties, interfacial interactions, and heat dissipation pathways within the multilayer stack.

Metallization studies provide another useful interface-level example. Copper coatings deposited by APS on

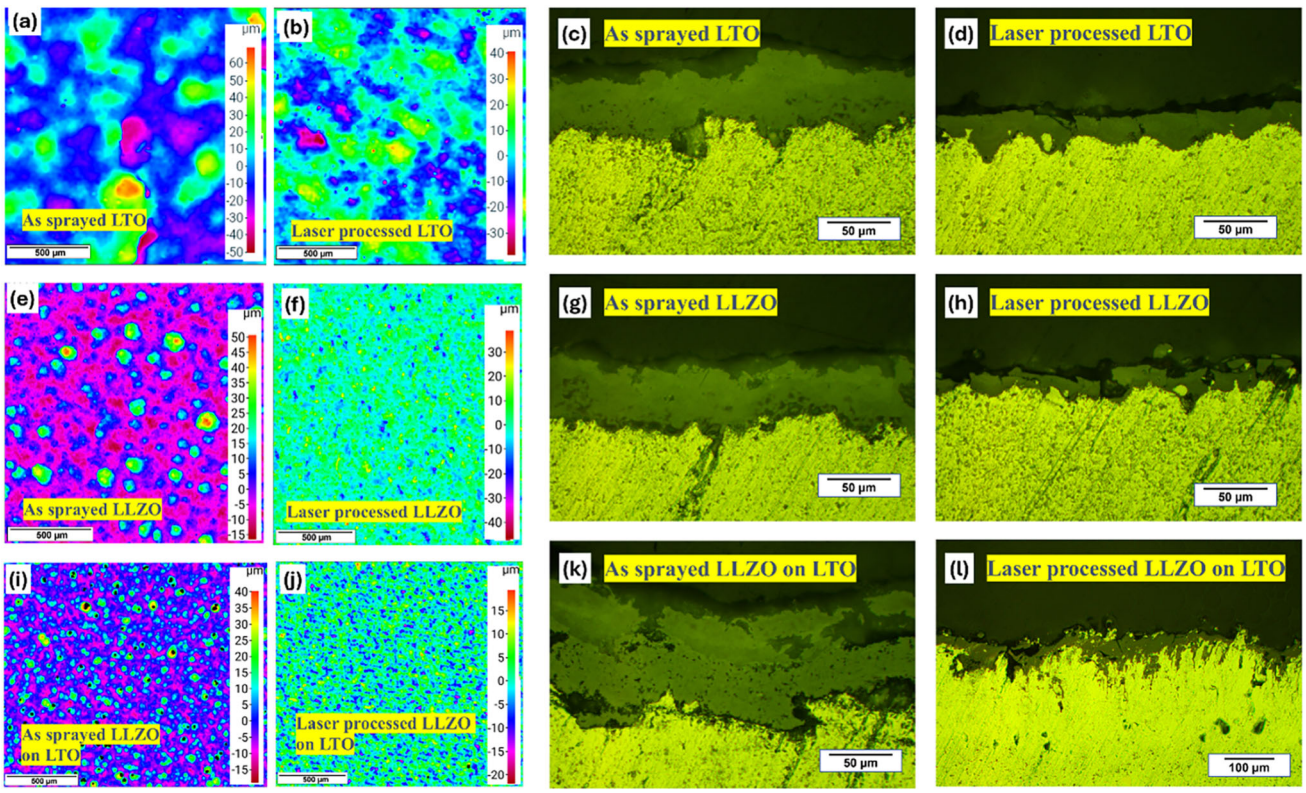

Fig. 7 Surface topography maps and cross-sectional microscopic images of as sprayed and laser processed coatings: (a-d) single-layer LTO thin-film, (e-h) single-layer LLZO thin-film, (i-l) double layer LLZO on LTO thin-film. Reprinted from (Ref 170), available under CC BY 4.0 license at ScienceDirect

garnet-type electrolytes formed robust, low-resistance interfaces, suggesting a possible scalable alternative to vacuum-deposited Cu in anode-free configurations (Ref 171). This addresses the formation of a metallic current–collector interface on the solid electrolyte, which is a necessary integration step for anode-free or hybrid solid-state battery architectures.

Another useful comparison is provided by LLZO–LCO cathode/electrolyte architectures fabricated by high-pressure field-assisted sintering (FAST), where a relative density of $\sim$ 95% was achieved. When assembled with a lithium metal anode, the dense architecture showed nearly twice the surface storage capacity of a comparable cell processed under lower pressure (Ref 172). Although this is not a thermal-spray demonstration, it reinforces the importance of densification and interfacial contact in oxide solid-state battery architectures.

Overall, these interface-focussed studies show that a thermally sprayed layer cannot be judged only by its depositability. Reliable integration into SSTFB stacks also requires control of surface quality, near-interface phase stability, densification, contact behaviour, and electrochemical response against adjacent cell components.

Multilayer and Full-Stack Demonstrations

Multilayer and full-stack demonstrations represent the most advanced stage of thermal-spray-based SSTFB development where individual functional layers (anode, solid electrolyte, and cathode) are sequentially integrated into device structures. At this level, the challenge shifts from depositing individual materials to integrating several functional layers without losing interface quality, phase stability, and transport continuity. Defects can also accumulate from one layer to the next. Roughness or porosity in a prior fabricated layer can affect new interfaces, while residual stress or local reaction zones may become more important as the architecture becomes more complex. A key proof-of-concept was the fabrication of APS-based layer-by-layer all-solid-state battery architecture, in which the anode, solid electrolyte, cathode, and current collector layers were sequentially deposited as functional layers (Ref 31). In this work, the LTO anode layer was first deposited on the Al current collector, followed by LLZO to form an anode|electrolyte architecture. The stack was then completed by depositing $LiNi_{1/3}Mn_{1/3}Co_{1/3}O_2$ (NMC111) as the cathode, producing an LTO|LLZO|NMC111 architecture. BSE cross sections and EDS spectra confirmed the presence of the intended LTO, LLZO, and NMC111 regions, with visually intact interfaces between the stacked layers, as shown in Fig. 8. However, electrochemical cycling of the full stack was not reported. The study should therefore be viewed as a structural proof-of-concept for sequential APS stacking rather than as a demonstration of full-cell battery performance. This is still an important demonstration because it shows that spray-based layer stacking is possible. At the same time, it should be treated as an early-stage architecture rather than a fully optimized SSTFB. Sequential spraying can introduce interlamellar porosity, rough interfaces, and phase changes that affect ionic transport and mechanical integrity across the stack. The main challenge is therefore not only stacking the layers, but also controlling how each deposition step modifies the layers and interfaces already present.

Processing Lessons from Thermally Sprayed SOFC Architectures

Useful manufacturing insight can also be drawn from the solid oxide fuel cell (SOFC) research. In SOFCs, thermal spray has been used for more than two decades to fabricate ceramic electrolytes, porous electrodes, metal-supported cells, and complete multilayer architectures. Dense yttria-stabilized zirconia (YSZ) electrolytes have been produced by APS (Ref 173), VPS, SPS, and related approaches, while porous electrode layers have been tailored through feedstock and process control (Ref 126, 174, 175).

A major focus in SOFC processing has been the production of thin electrolyte layers with low gas leakage, while maintaining high deposition rates and avoiding prolonged high-temperature sintering (Ref 176, 177). This is directly relevant to sprayed SSTFB development because the same processing tension appears there in a different form. The electrolyte layer must be continuous and defect-controlled, but the process also needs to remain scalable. SOFC studies show that this balance is governed by how the coating forms during deposition: splat-boundary defects can become leakage paths, and poor electrode–electrolyte contact can increase interfacial resistance. Feedstock size, particle melting, substrate temperature, and thermal history therefore become part of the electrochemical design, not only the coating process (Ref 176-178). Insights from metal-supported SOFCs are also useful, as they show that sequential spray deposition can be used to build electrochemical multilayers on mechanically robust substrates. These studies can serve as guidelines for thinking about thermal-sprayed SSTFB stacks, where the substrate is not only a support but also affects adhesion, residual stress, interface formation, and the allowable post-treatment window (Ref 179-181).

This comparison, however, comes with important limitations. SOFCs operate at much higher temperatures than SSTFBs and usually tolerate thicker layers, different defect populations, and different interface chemistries. This changes how electrolyte quality has to be judged. A defect population that may be acceptable in a thick SOFC

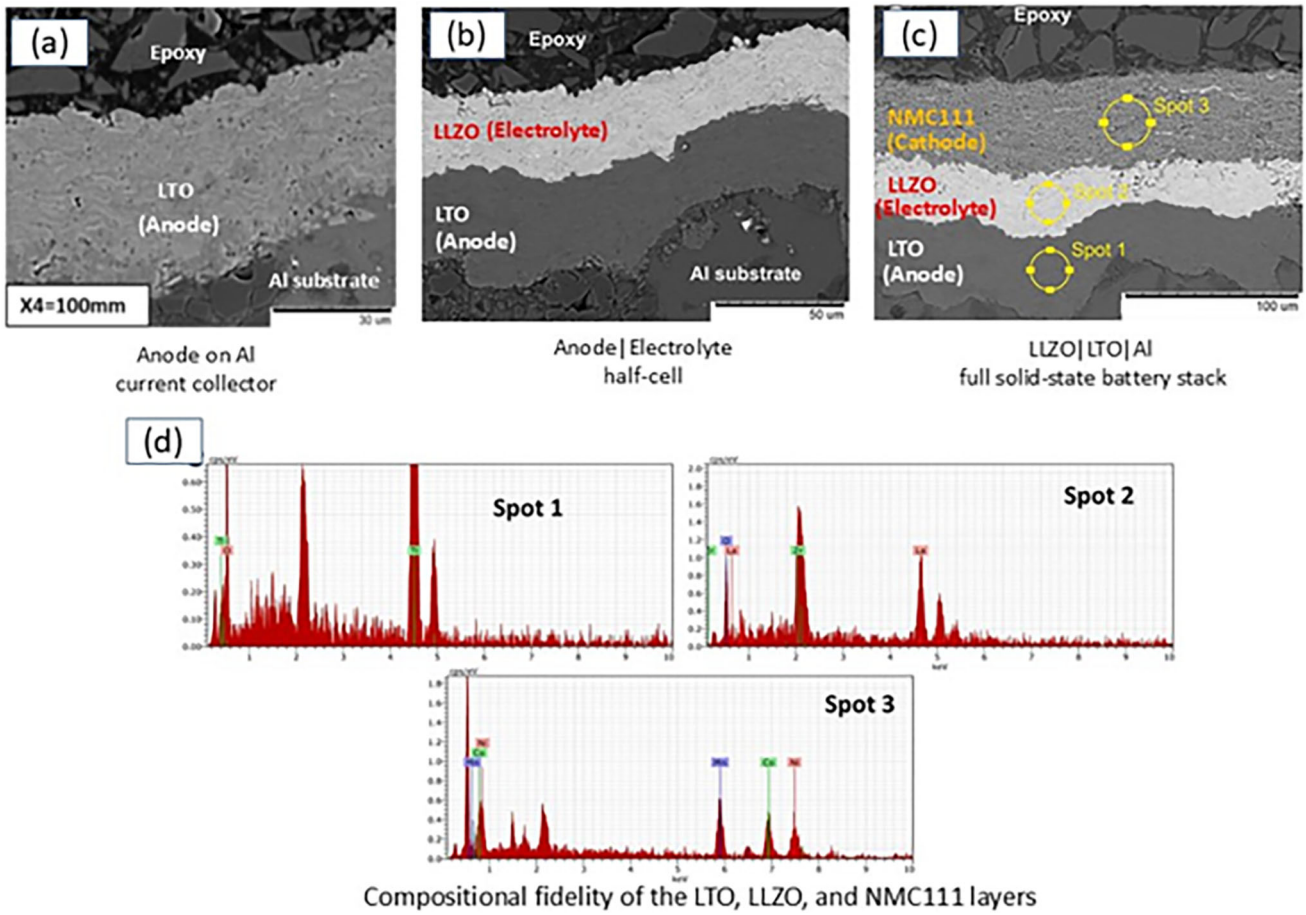

Fig. 8 Cross-sectional BSE micrographs of sequentially deposited battery constituents fabricated by atmospheric plasma spraying (APS): (a) $Li_4Ti_5O_{12}$ (LTO) anode layer on Al current collector; (b) $Li_7La_3Zr_2O_{12}$ (LLZO) solid electrolyte deposited on LTO, forming an anodelelectrolyte architecture; and (c) $LiNi_{1/3}Mn_{1/3}Co_{1/3}O_2$ (NMC111) cathode deposited on the LLZO|LTO|Al stack. (d) EDS spectra collected from representative regions of the LTO, LLZO, and NMC111 layers. Reprinted from (Ref 31), available under CC BY 4.0 license at ScienceDirect. The figure demonstrates structural feasibility of sequential APS stacking, while electrochemical cycling of the full stack was not reported

electrolyte can become more critical in an SSTFB electrolyte, where the layer is much thinner, must block electronic leakage over short transport distances, and must remain compatible with lithium-containing electrodes. Therefore, while SOFC results cannot be transferred directly to SSTFBs, but learnings can be translated from a more practical standpoint: they show which processing variables become critical when dense ceramic electrolytes, porous electrodes, metallic supports, and multilayer interfaces are produced by thermal spray-based routes. These lessons can guide thermal-spray-based SSTFB development, but do not eliminate the need for battery-specific validation.

Characterization-Led Insights into Process-Induced Heterogeneity

The need for battery-specific validation becomes especially clear when thermally sprayed layers are examined at smaller length scales. Thermal spray processing can produce spatially heterogeneous battery layers because particles or droplets experience different heating, melting, impact, cooling, and reheating histories during deposition. For SSTFB-relevant coatings, this can produce local variations in lithium content, phase composition, porosity, or interface chemistry. These can, in turn, strongly affect ionic transport, electronic leakage, interfacial resistance, and cycling stability. Classical coating characterization metrics, such as porosity, adhesion, hardness, and average phase analysis, are therefore useful, but not sufficient on their own.

Recent work shows why spatially resolved characterization is needed. Synchrotron-based techniques such as μXRD, μXRF, and x-ray absorption spectroscopy can map local phase distributions, elemental gradients, and redox-state changes within thermally sprayed battery coatings (Ref 32, 135, 182). When combined with in situ or operando electrochemical testing, these methods can also help connect spray parameters, local microstructure, and degradation behaviour more directly. For example, synchrotron μXRD/μXRF analysis of sprayed LTO coatings showed that the spinel phase may be retained overall, while lithium-depleted secondary phases can still form locally near interfaces or splat boundaries (Ref 29). Similar approaches are useful for LLZO-based coatings, where surface smoothing or laser remelting may reduce roughness but can also introduce local oxidation or phase changes (Ref 32).

The broader solid-state battery literature offers useful tools for studying these problems, even when the studies are not thermal-spray-specific. Synchrotron x-ray methods, including operando x-ray tomography, have been used to follow structural and morphological changes in solid-state battery systems (Ref 183, 184). Neutron-based methods provide complementary sensitivity to light elements and have been applied through neutron imaging, neutron scattering, and neutron reflectometry to probe lithium redistribution, transport constraints, and buried interfacial evolution (Ref 185-189). Focussed ion beam SEM and related correlative imaging methods are useful for linking defects, pores, cracks, and interface morphology across different length scales (Ref 190). Solid-state NMR provides local structural and dynamic information, particularly for ion environments, transport, and interfacial species (Ref 183). Cryogenic electron microscopy and other high-resolution methods can further help preserve and examine reactive or beam-sensitive interphases, although a specific thermal-spray-relevant example is still needed here (Ref 191). These studies are relevant to thermally sprayed SSTFB layers, because they are also likely to fail through similar buried-interface, local-composition, and defect-mediated mechanisms.

For thermally sprayed SSTFB layers, characterization should therefore resolve both the coating scale and the local defect scale. Through-thickness phase and composition gradients should be monitored because different coating regions experience different thermal histories. Splat boundaries, interfaces, and reheated regions need closer attention as they are likely sites for alkali depletion, secondary phase formation, or localized decomposition. Interfaces also require chemical analysis, since diffusion or reaction zones can introduce resistive phases and increase charge-transfer resistance. Finally, porosity, splat bonding, residual stress, and coating integrity should be assessed together, because a coating that appears continuous in cross section may still contain connected defects or stress-induced damage that affects transport during cycling.

The main value of these techniques is that they move the assessment beyond average coating properties. For thermal-spray-based SSTFBs, future studies should combine coating-scale measurements with spatially resolved chemical, structural, and electrochemical characterization. This will help distinguish successful coating deposition from genuinely functional battery-layer fabrication.

The characterization approaches discussed above are summarized in Table 2, together with selected examples from thermal-spray and broader solid-state battery studies.

Summary of Demonstrated Progress

The studies summarized in Table 3 show that thermal spray can fabricate functional battery-relevant layers, including LTO anodes, LCO cathodes, LLZO/LLZTO and LPO electrolyte candidates, metallic interlayers, and early multilayer stacks. The strongest evidence is currently at the single-layer level. LTO provides a useful model for understanding how lithium volatility, phase retention, and local decomposition affect sprayed oxide electrodes. LCO demonstrates the benefit of rapid active-material build-up, but also shows that post-annealing may be needed to recover the electrochemically active layered structure. Garnet and phosphate electrolytes show that dense and conductive ceramic coatings can be produced, although electrolyte performance remains sensitive to phase purity, residual porosity, and post-treatment. Metallic interlayers appear closer to practical use because they are less sensitive to spray-induced compositional changes than lithium-containing active materials.

At the architecture level, the most important progress is that sequential spray deposition is possible. However, device-level validation remains limited. Functional activity must be interpreted together with phase composition, local stoichiometry, interface quality, and post-treatment history. In some cases, electrochemical behaviour may arise from the intended phase; in others, it may also be influenced by metastable structures, secondary phases, local lithium depletion, or laser/annealing effects. To improve clarity and comparability across studies, it is important to report electrochemical performance together with local composition, phase distribution, interface quality, and reproducibility. To summarise, thermal spray should be viewed as a promising but still developing manufacturing route for selected SSTFB layers and hybrid architectures. Its near-term value is likely to be strongest where rapid material build-up, binder-free deposition, or metallization provides a clear manufacturing advantage. Conductive interlayers and partially integrated sprayed stacks may therefore be

Table 2 Selected examples of characterization methods to assess process-induced heterogeneity and buried interfaces relevant to thermally sprayed SSTFB layers

Year	Material/system	Characterisation method	Key result	References
2026	Sodium batteries	Multiscale characterization	Correlated interfacial transformations to mitigate space-charge resistance.	(Ref 192)
2026	All-solid-state lithium metal batteries, ASSLMBs	Multi-modal probes	Integrated temporal, spatial, and energy-resolved tools for dynamic analysis.	(Ref 191)
2026	$Li_4Ti_5O_{12}$, (LTO)	Synchrotron μXRD, SEM/EDS, XPS	Correlated thermal spray parameters with phase stability and lithium loss.	(Ref 163)
2025	All-solid-state batteries	In situ x-ray tomography & neutron scattering	Resolved multi-length scale interfacial volume fluctuations and void formation.	(Ref 184)
2025	All-solid-state batteries	Neutron imaging, x-ray tomography, focussed ion beam scanning electron microscopy, and cryogenic electron microscopy	Reveals microstructural and chemical changes in ASSBs at scales from the atomic to the macroscopic level, focus on the elusive failure behaviours at lithium anodes, strengths and limitations of each technique	(Ref 190)
2025	$Li_4Ti_5O_{12}$, (LTO)	Synchrotron μXRD and μXRF	Identified LTO phase retention and secondary phases near the interface.	(Ref 29)
2025	LLZO electrolyte	synchrotron μXRD	Laser remelting reduced surface roughness and lowered interfacial resistance.	(Ref 32)
2024	All-solid-state batteries	Neutron scattering, NPD, INS, QENS, SANS, NR, etc.	Provided a suite-wide overview of how neutron techniques resolve atomic-scale processes.	(Ref 185)
2023	Li metal/Lipon/NiO	In situ neutron reflectometry, NR	Measured buried solid-solid interfaces with nanometre-level precision.	(Ref 186)
2023	WO_X/electrolyte	In situ neutron reflectometry, NR	Probed liquid electrolyte and SEI structures; validated applicability to interface studies.	(Ref 187)
2020	Solid-state Li-ion batteries	Synchrotron x-ray & solid-state NMR, neutron scattering	Decoupled lithium distribution variations within solid composite architectures.	(Ref 183)
2015	Silicon anode	In situ neutron reflectometry	Directly measured SEI thickness and composition vs. state of charge.	(Ref 188)
2014	$LiMn_{1.5}Ni_{0.5}O_4$ cathode	In situ neutron reflectometry	Determined interface thickness and composition evolution.	(Ref 189)

Table 3 Summary of research on SSTFB-related layers manufactured by thermal spray

Material/system	Thermal spray process	Substrate	Key phases/microstructure	Electrochemical characteristics/highlights	Layer thickness, μm	References
$Li_4Ti_5O_{12}$ (LTO)	APS (powder feed)	SS	Mixed LTO + TiO_2; lamellar	Exhibited ~ 1.55 V plateau; confirmed Li storage activity despite partial TiO_2	Not reported	(Ref 161)
Li_4Ti5O_{12} (amorphous)	APS (rapid quench)	SS	Amorphous film	Structural relaxation after cycling; stable quasi-solid-state operation.	~ 5-8(from FIB cross section)	(Ref 162)
$Li_4Ti_5O_{12}$ (LTO)	SPS (suspension feed)	SS	~ 76 wt.% spinel LTO + minor TiO_2	Reversible lithiation/delithiation; binder-free thin film validated SPS feasibility	~ 12-50 (for various parameters)	(Ref 124)
$Li_4Ti_5O_{12}$	SPS	SS 304	Spinel LTO dominant; $Li_2Ti_3O_7$/ Li_2TiO_3 near interface	Identified local Li depletion zones; emphasized need for process optimization.	~ 40	(Ref 29)
TiO_2/$Li_4Ti_5O_{12}$ dual layer	APS (powder feed)	SS foil	Nanocrystalline TiO_2 + spinel LTO	Demonstrated all-active-material electrode concept; tunable capacity by spray energy.	TiO_2 ~ 523 average; LTO not reported	(Ref 135)
$LiCoO_2$ (LCO)	APS (high-deposition-rate)	Al foil	Layered structure partially degraded; recrystallized after anneal	Thick, > 5 µm LCO films; areal capacity > 5 mAh cm^{-2} after post-anneal.	Multiple thicknesses; up to 130	(Ref 164)
LTO, LLZO, NMC111	APS	Al	APS (multi-layer build)	Sequential APS stacking of LTO, LLZO, and NMC111 was shown structurally; electrochemical cycling of the full stack was not reported.	LTO anode ~ 40; LLZO electrolyte ~ 40; NMC111 cathode Highly SoD-dependent; ~ 9-18	(Ref 31)
Si composite anode	Supersonic cold spray	Cu/Al	Work-hardened, dense Si-alloy splats	Viable Li-ion anode via solid-state spray; preserves chemistry	Not reported	(Ref 193)
$La_{0.8}Sr_{0.2}Ga_{0.8}Mg_{0.2}O_3$ (SOFC electrolyte)	HVOF	SS	Dense spinel/oxide structure; controlled volatility	Demonstrates viability of lower-enthalpy HVOF for spinel-type cathodes	LSGM ~ 60; LSGM in SOFC cell 50-55	(Ref 165)
$Li_7La_3Zr_2O_{12}$ (LLZO)	APS (large-area)	Al_2O_3	Cubic LLZO; dense ~ 300 µm film	$\sigma = 3.8 \times 10^{-5}$ S cm^{-1} (after anneal; flexural strength ≈ 157 MPa)	LLZO 30-300	(Ref 141)
$Li_{6.5}La_3Zr_{1.5}Ta_{0.5}O_{12}$ (LLZTO)	SPS (suspension)	SS 304	~ 68% cubic phase; ~ 75% crystallinity	$\sigma \approx 10^{-8}$ S cm^{-1} (as-sprayed; dense nanostructure)	LLZTO-1 17 ± 1; LLZTO-2 16 ± 3; LLZTO-3 20 ± 3	(Ref 166)
Li_3PO_4 (LPO)	APS	SS Substrate	Dense γ-LPO, < 1% porosity; Li/P > 3	$\sigma \approx 4.6 \times 10^{-8}$ S cm^{-1}; γ-phase stability without post-anneal	200-300	(Ref 167)
$Na_3Zr_2Si_2PO_{12}$ (NZSP/NASICON)	APS	Al_2O_3	Dense NZSP electrolyte layer, Na, P evaporation during spraying, annealing required	$\sigma \approx 1.93 \times 10^{-4}$ S cm^{-1} at 200 °C after annealing at 1000 °C, shows electrolyte-level thermal spray feasibility beyond Li systems	~ 100	(Ref 144)
Cu metal (interlayer)	APS	LLZO ceramic	Dense, low-oxide Cu film	Robust low-resistance interface on garnet electrolytes	~ 20	(Ref 171)

Table 3 continued

Material/system	Thermal spray process	Substrate	Key phases/microstructure	Electrochemical characteristics/highlights	Layer thickness, μm	References
$Li_4Ti_5O_{12}$	APS	SS 304	Laser processing to decrease surface roughness	surface roughness decreased, no significant change in chemical composition, oxygen % increased	Not reported	(Ref 194)
LLZO	SPS	Aluminium	Laser processing to decrease surface roughness	surface roughness reduced by 40%, localized oxidation and phase transformation after laser processing	35 ± 5	(Ref 32)
LTO, LLZO, bilayer (LLZO on LTO)	SPS	Aluminium	Laser processing to decrease surface roughness	Mainly a post-processing/interface study; no electrochemical performance reported. Optimized laser parameters for single layers could not be directly transferred to the bilayer, where severe ablation of both layers was observed.	LTO ~ 40; LLZO ~ 40	(Ref 170)

more realistic early targets than complete SSTFB devices. Broader adoption of thermal spray in SSTFB manufacturing will depend on better control of both chemistry and coating quality. Lithium retention and phase stability must be improved, while roughness, defect formation, interfacial reactions, and electrochemical reproducibility need to be controlled more reliably.

Comparative Assessment and Manufacturing Challenges

Benchmark Comparison of Conventional SSTFB Routes and Thermal Spray

Table 4 summarizes the main differences between established SSTFB manufacturing routes and thermal spray. Conventional vacuum-based methods such as sputtering, PLD, and ALD remain the most suitable routes when ultrathin, smooth, dense, and compositionally controlled films are required. They are especially important for pinhole-free electrolytes, precisely engineered interfaces, and model thin-film architectures. Their limitations are mainly related to deposition rate, equipment cost, coating area, and scalability.

Thermal spray offers a different set of advantages. Its value lies in rapid material build-up, flexible coating thickness, larger-area deposition, lower dependence on vacuum infrastructure, and compatibility with powder, suspension, or solution precursor feedstocks. These attributes make it relevant for selected SSTFB layers where throughput, thickness, or binder-free deposition is more important than sub-micrometre thin-film precision. Thermal spray should therefore not be viewed as a direct replacement for sputtering, PLD, or ALD across the entire battery stack. A more realistic role is as part of a hybrid manufacturing route, where each process is used to fabricate a layer for which it is the most appropriate. In such a strategy, thermal spray could be used to build suitable electrode, electrolyte, current-collector, or interlayer structures at higher rates, while other methods are used to correct or refine the features that thermal spray does not control well. For example, sputtering or ALD could be used to introduce ultrathin interlayers that improve interface chemistry, suppress side reactions, or reduce interfacial resistance (Ref 29, 111, 195). Localized laser treatment could be adopted to smooth rough sprayed surfaces, close near-surface porosity, or modify crystallinity without reprocessing the full coating thickness (Ref 32, 194, 196). This type of multi-stage, multi-process route is more practical than expecting any single fabrication route to satisfy all requirements of a complete SSTFB stack. Where thermal spray does not provide sufficient surface quality or

Table 4 Comparison of various attributes of manufacturing routes for SSTFBs

Parameter	Sputtering, PVD	Pulsed Laser Deposition, PLD	Sol–Gel Coating	ALD/CVD	2D Printing, Inkjet/Screen	Thermal Spray
1 Throughput and deposition rate						
Deposition rate	0.02-0.2 μm/h, RF; up to ~ 2 μm/h, DC	1-100 nm/s; area limited	0.5-10 μm per coat; fast spin/dip; slow pyrolysis	0.02-0.13 Å/cycle; ~ 1-10 nm/h practical	1-50 μm/pass, screen; 0.1-5 μm/pass, inkjet	Tens–hundreds μm/min; 1-45 kg/h mass rate
Typical film thickness range	0.1-5 μm	0.1-2 μm	0.5-10 μm, post-anneal	0.05-1 μm, ideal < 100 nm	2-200 μm, post-sintering	20 μm–several mm
Coating area/substrate size	Up to 300 mm; roll-to-roll feasible, vacuum	Historically small; recently scaled to 300 mm	Large area; spin, dip, spray applicable	Conformal on 3D; batch: 50-100 wafers	Large area; flexible substrates; roll-to-roll	large-area capability; no vacuum chamber for atmospheric variants; portable
Scalability to industrial production	Low–medium	Low—research scale only	High—simple equipment; large-area coatable	Medium	Very high	Very high
2 Material utilisation						
Material utilisation efficiency	Low—20-40%; target erosion; chamber losses	Very low— < 5%; plume divergence losses	Moderate —60-80%; sol wastage during coating	Near 100% in ALD window, self-limiting	Moderate—50-80%, screen; 30-60%, inkjet	40-60%, conv. APS, process dependent
Primary waste mechanism	Target erosion; off-substrate chamber coating	Plume divergence; off-axis particle losses	Cracking/shrinkage during drying & sintering	Precursor purging; unreacted precursor waste	Ink overflow; misalignment; sintering losses	Overspray; rebound of unmelted particles
Vacuum/ atmosphere requirement	Yes—10^{-3} to 10^{-6} mbar; high infrastructure	Yes—10^{-6} to 10^{-8} mbar; most stringent	No—ambient atmosphere	Yes, thermal ALD; spatial ALD → atmospheric	No—ambient atmosphere	Process dependent: Fully atmospheric in APS, controlled atmosphere in VPS
3 · Thermal operations						
Processing temperature, substrate, °C	300-600, post-annealing often needed	400-700 for crystalline films	400-800, pyrolysis/ sintering required	Room temp–200, ALD; 200-500, CVD	25-200, printing; > 600, sintering	Substrate < 150 despite plasma > 12,000
4 FILM quality and density						
Film density/porosity	Very high density; < 1% porosity	Very high; epitaxial quality possible	Moderate—porous unless annealed; cracking risk	Highest conformality; pinhole-free at < 15 nm	Moderate—porosity reduces after sintering	Controllable by APS and HVOF
Stoichiometry control	Good; reactive sputtering enables tuning	Excellent—congruent stoichiometric transfer	Good—composition tunable via precursor ratio	Excellent—atomic-level self-limiting control	Moderate—ink composition governs	Moderate—rapid solidification; phase changes possible
Reported ionic conductivity achieved for solid electrolytes, S cm^{-1}	10^{-6}-10^{-5}	10^{-5}-10^{-4}	10^{-5}-10^{-4}, post-annealing	10^{-5}-10^{-4}	10^{-4}-10^{-3}, post-sintering	10^{-5}-10^{-3}, process-dependent and emerging
Film uniformity & conformality	Good; uniform over planar substrates	Good in a small area; drops off at edges	Moderate—drying gradients cause non-uniformity	Excellent—self-limiting; conformal on 3D	Moderate—resolution limited ~ 20-50 μm	Good for planar; line-of-sight limitation

Table 4 continued

Parameter	Sputtering, PVD	Pulsed Laser Deposition, PLD	Sol–Gel Coating	ALD/CVD	2D Printing, Inkjet/Screen	Thermal Spray
5 COST implications						
Relative capital/ equipment cost, CAPEX, USD	High—$500 K-$2 M, industrial tools	Very high—$500 K-$3 M	Very low— < $50 K; basic lab equipment	High—$300 K-$2 M;	Low–moderate—$50 K-$500 K	Low–moderate—$100 K-$500 K; no vacuum
Relative operating cost, OPEX	High—vacuum pumping; target replacement	Very high—laser consumables; low throughput	Low—precursor chemicals; furnace energy	High—precursor cost; long cycle times	Low—ink cost; fast printing; ambient	Low–moderate—gas/fuel; powder feedstock
Relative cost per m^2 of coating	High	Very high—slowest area coverage; research only	Low—simple process; low-cost precursors	High	Low—dominant cost is ink formulation	Low—rapid mass deposition; no vacuum OPEX
Overall suitability for scalable SSTFBs manufacturing	R&D standard; high quality; poor throughput	Research tool only; not scalable	Low cost; scalable; film quality and Li loss at sintering are key limits	Ideal for ultra-thin electrolyte interlayers only	High scalability; suitable for thick electrodes	High scalability potential; usefu l where higher thickness or areal loading is acceptable

The values are approximate literature-based ranges and may vary with material system, equipment configuration, coating thickness, substrate geometry, and post-treatment requirements. References for this table can be found in supplementary table S1.

defect control on its own, post-deposition steps such as laser smoothing, sealant infiltration, or ultrathin PVD/ALD interlayers may also be needed as part of a hybrid manufacturing route. However, hybrid processing must be considered carefully, as every additional technique brings its own equipment, process-control, handling, and quality-assurance requirements. The complexity can become substantial when several distinct processes are combined in one manufacturing sequence, so such routes must be evaluated not only for materials compatibility but also for cost, throughput, process integration, and scalability.

The comparison also shows that scalability should not be assessed only in terms of deposition rate or coating area. Material utilization is equally important. Thermal spray is not inherently a low-waste process, since overspray, rebound, and filter dust represent a significant fraction of unutilized feedstock. This becomes especially relevant for battery materials containing expensive or strategically important elements such as lithium, cobalt, niobium, or rare earths. Therefore, deposition efficiency, overspray recovery, feedstock recycling, and contamination control must be considered alongside throughput and cost when assessing thermal spray for SSTFB manufacturing. These issues are closely linked to the broader manufacturing challenges discussed below, including composition retention, process cleanliness, microstructural control, and reproducibility.

Key Manufacturing Challenges for TS-Enabled SSTFBs

Scaling thermal-spray-enabled SSTFBs requires more than showing that battery materials can be deposited. The central manufacturing question is whether the process can produce reproducible battery-layer function while maintaining throughput, material utilization, and stack compatibility. The demonstrations discussed above show that this is possible in selected cases, but they also define the process controls that will be needed for broader use.

One of the main issues is chemistry retention. Lithium/sodium-containing oxides are sensitive to high-temperature exposure because Li/Na can volatilize during in-flight heating, splat formation, or subsequent reheating. Oxygen stoichiometry and cation distribution can also change during spraying, especially in multicomponent oxides or phase-sensitive electrode and electrolyte materials (Ref 30, 144). These changes do not necessarily remove electrochemical activity, but they can shift the coating away from the intended material design. For SSTFB layers, this matters because conductivity, voltage response, and interfacial stability are closely linked to phase purity and local stoichiometry. Feedstock design, plasma enthalpy, residence time, atmosphere, and substrate temperature

therefore need to be treated as chemistry-control variables, not only as coating-formation parameters.

A second requirement is electrolyte defect control. In many conventional coating applications, a dense ceramic layer can still be acceptable when it contains some splat boundaries, isolated pores, or microcracks. SSTFB electrolytes have a lower tolerance for such defects because they must support ionic transport while blocking electronic leakage and short-circuit pathways. Connected porosity, unbonded splat boundaries, through-thickness cracks, and local thickness variations are therefore critical features to control. This does not make sprayed electrolytes impossible, but it does mean that coating density alone is not a sufficient benchmark. Electrolyte layers need to be assessed in terms of both microstructure and functional transport. Surface roughness and interface formation are closely linked to this issue. Sprayed coatings often develop rough or nodular surfaces because of splat stacking, shadowing, partially reacted droplets, or heterogeneous melting. Such surface features may be acceptable, or even useful, in some electrode architectures. They are more difficult to accommodate when the next layer must form a clean and continuous electrochemical interface. Roughness can propagate through the stack, affect local current distribution, and increase the area available for parasitic reactions. For this reason, surface conditioning is likely to be important in sprayed SSTFB architectures, particularly for electrolytes and buried interfaces.

Hybrid mitigation strategies may help address this limitation. Thermal spray could provide the main layer thickness and architecture, while post-deposition steps improve the functional surface. Laser smoothing, sealant infiltration, sol–gel-derived surface layers, or ultrathin PVD/ALD interlayers could help reduce open porosity, smooth asperities, or improve contact between adjacent layers (Ref 197, 198). These treatments should not be viewed as corrections for a failed coating, but as part of a realistic process chain. For electrolyte layers, any infiltrated or overcoated phase should ideally remain ionically conductive and electronically insulating. For electrodes and current collectors, it must at least be electrochemically benign and stable during cycling.

Process cleanliness is a more practical, but equally important, issue. Thermal spray is usually carried out in industrial coating environments, whereas battery fabrication often requires stricter control over moisture, oxygen exposure, particulates, and cross-contamination. This is especially relevant for lithium-containing materials, sulphides, and other air- or moisture-sensitive chemistries. Adapting thermal spray for SSTFB manufacturing may therefore require controlled-atmosphere spraying, enclosed deposition cells, glovebox-compatible handling, or dedicated powder and overspray-management protocols. These adaptations would add complexity, but they may also make thermal spray more compatible with battery manufacturing requirements.

The final issue is reproducibility. SSTFB performance depends on several coupled factors, including phase composition, local stoichiometry, density, surface roughness, interface quality, and post-treatment history. Small changes in spray conditions can affect several of these factors at once. Future studies should therefore report not only electrochemical response, but also deposition efficiency, coating uniformity, local chemistry, defect distribution, and repeatability across samples.

Overall, the manufacturing challenge is not simply to make thermal spray coatings thinner or denser. It is to define process windows where chemistry, microstructure, interface quality, cleanliness, and reproducibility are controlled well enough for the intended layer function. This does not exclude thermal spray from SSTFB manufacturing. Rather, it suggests that its strongest role may be in selected layers, conductive interlayers, metallization, and hybrid architectures where its deposition-rate and material-build-up advantages can be used without forcing it to meet every requirement of conventional thin-film processing.

Minimum Reporting Standards for Thermally Sprayed Battery Layers

Thermal spray has a strong industrial background in aerospace, energy, biomedical coatings, and SOFC manufacturing, where robotic handling, large-area deposition, and high-throughput coating production are already established. However, this experience cannot be transferred directly to SSTFB manufacturing. Battery layers place stricter demands on chemistry, contamination control, interfaces, and reproducibility than many conventional thermal spray applications. Even small amounts of impurity pickup, local phase gradients, residual porosity, roughness, or interfacial resistance can strongly affect electrochemical performance.

For this reason, progress in thermal-sprayed SSTFB layers should be assessed carefully in terms of film quality and performance. At this stage, the field does not yet need rigid qualification standards, but would benefit from a common minimum reporting framework. Without this, it is difficult to compare results across studies or to judge whether thermal spray is moving towards reproducible battery-layer fabrication rather than isolated proof-of-concept demonstrations.

Such a framework should therefore go beyond spray parameters alone. Future studies should report information covering feedstock characteristics, spray conditions, coating geometry, surface and microstructural features, phase composition, interface quality, electrochemical testing

protocol, reproducibility, and manufacturing relevance. This is especially important for electrolyte layers, where film density, open porosity, pinhole statistics, electronic leakage, and interfacial resistance are as important as ionic conductivity. Similarly, for electrodes and current collectors, reporting should include not only electrochemical performance, but also adhesion, roughness, connectivity, post-treatment conditions, and compatibility with subsequent layers.

The recommended minimum parameters are summarized in Table 5. These parameters are intended as a first step towards building a shared basis for process validation, cross-laboratory comparison, and eventual standardization of thermal spray-based SSTFB manufacturing. A combined reporting of coating quality, electrochemical performance, reproducibility, and material utilization will be needed before thermal-sprayed battery layers can be fairly benchmarked against PVD, ALD, solution-based, printing, or other conventional manufacturing routes.

Conclusions and Outlook

The performance of solid-state thin-film batteries is strongly dependent on how each layer is manufactured. This is particularly controlled not only by the choice of electrode or electrolyte material, but also by thickness, roughness, composition retention and phase purity of each layer, as well as by film continuity and interface quality. Conventional vacuum-based routes such as sputtering, PLD, evaporation, ALD, and CVD can produce dense, smooth, and compositionally controlled films, especially for solid electrolytes and interfacial layers, and will continue to be useful for fundamental studies, model interfaces, and precision thin-film stacks. However, their practical limitations, viz. low deposition rates, high infrastructure cost, and restricted area scalability, make them inappropriate for higher-throughput manufacturing. Solution-based and printing routes address some of these limitations, but they introduce other problems related to drying, binder removal, shrinkage, cracking, lithium loss, and post-deposition densification. Overall, a single scalable deposition route that satisfies all SSTFB requirements continues to be elusive.

Thermal spray adds a different capability to this manufacturing space. It offers high deposition rates, flexible thickness build-up, large-area coating capability, and compatibility with powder, suspension, and solution precursor feedstocks. These features make it attractive for selected SSTFB components, particularly where thicker functional layers, current collectors, graded structures, protective coatings, or scalable deposition are required. Reported studies on thermally sprayed SSTFB-relevant materials have already shown that thermal spray is not merely a conceptual option. Several individual components, including oxide electrodes, oxide solid-electrolyte candidates, metallic current collectors, and interlayers, have already been deposited using appropriate thermal spray variants.

However, this does not imply that thermal spray can replace established thin-film methods across the entire battery stack. Successful coating deposition must be distinguished from device-level validation, especially for electrolyte layers and multilayer stacks where density, interfacial resistance, phase stability, and cycling performance must be demonstrated together. The same

Table 5 Minimum reporting parameters proposed for thermal-sprayed functional battery layers

Category	Minimum parameters to report
Feedstock	Composition, particle/droplet size distribution, precursor chemistry, solvent, impurity level
Spray process	Process type, torch/nozzle, power, gases, feed rate, spray distance, atmosphere, substrate temperature, number of passes
Film geometry	Thickness, thickness uniformity, coating area
Surface and microstructure	Roughness, total porosity, open and closed porosity, pore size, crack density, splat/columnar features
Chemistry and phase	Phase purity, secondary phases, through-thickness gradients, Li/Na/ volatile-element retention, impurity uptake
Interface quality	Interfacial roughness, reaction layers, interdiffusion, adhesion/cohesion, residual stress where relevant
Electrochemical data	Ionic/electronic conductivity, interfacial resistance, voltage window, current density, cycling protocol, temperature, stack pressure
Reproducibility	Number of samples, mean ± standard deviation, failure rate/yield, batch-to-batch variability
Manufacturing relevance	Deposition rate, deposition efficiency/material utilization, overspray fraction, post-treatment steps, scalability assumptions

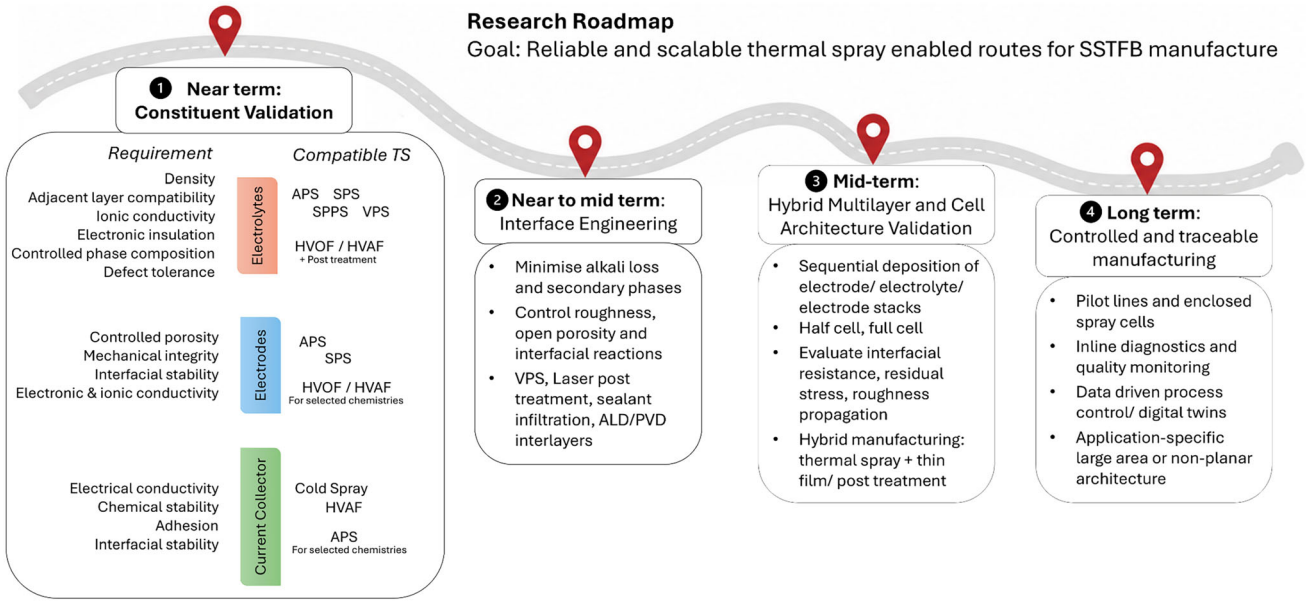

Fig. 9 Research roadmap for developing thermal-spray-enabled SSTFB manufacturing. The near-term stage focuses on constituent validation of individual electrolytes, electrodes, current collectors, and interlayers by matching layer requirements with suitable thermal spray processes. Subsequent stages address interface engineering, hybrid multilayer and cell-architecture validation, and controlled and traceable manufacturing using enclosed or partially enclosed spray systems, inline diagnostics, quality monitoring, and data-driven process control. The roadmap emphasizes progression from layer-level feasibility towards integrated stack validation and manufacturing control

deposition mechanisms driven by favourable thermal and kinetic conditions that enable rapid coating formation can also cause residual porosity, rough surfaces, residual stresses, contamination, and interfacial reactions in case of material-process incompatibility. Lithium/sodium-containing battery materials add another constraint, as excessive heat input can lead to alkali volatilization, phase decomposition, compositional drift, and loss of ionic transport, particularly in garnet-, spinel-, or compositionally complex oxide systems. Therefore, appropriate TS process selection is critical. Lower-temperature routes, controlled-atmosphere spraying, and liquid-feedstock processes such as SPS and SPPS may help reduce thermal damage, improve compositional control, and deliver finer microstructures. In many cases, these approaches may need to be combined with appropriate post-treatments to achieve careful microstructural and interfacial control, reduce open porosity, and improve surface continuity, resulting in better electrochemical performance.

The need to align spray conditions with SSTFB layer requirements also points to a broader opportunity in process–material design. Future progress is unlikely to come from simply forcing conventional SSTFB materials into thermal spray processing windows. A more realistic route is to identify layers where thermal spray offers a genuine processing advantage and then adapt feedstock chemistry, particle or precursor design, and layer architecture to exploit those advantages while still meeting SSTFB functional requirements. As an illustrative example, compositionally complex oxides, including high-entropy oxides (HEOs), are interesting in the context of SSTFBs because their phase stability, defect chemistry, and multi-cation redox behaviour may offer useful design flexibility (Ref 199, 200). Most conventional HEO synthesis routes rely on mixing individual oxide powders, often by ball milling, followed by high-temperature sintering. Liquid-feedstock routes such as SPPS offer a uniquely different pathway that involves molecularly mixed precursors and bypasses the time- and cost-intensive powder-synthesis step. This could be useful for producing homogeneous multi-cation coatings that are difficult to obtain by conventional powder processing (Ref 201). Of course, thermal spray processing of HEOs comes with its own challenges—difficulty of retaining multicomponent chemistry during spraying, including preferential volatilization of certain elements, phase segregation, incomplete mixing, and composition drift, which are active research questions. For SSTFBs, the use of HEO-type materials is still at an early stage and will require careful benchmarking of phase stability, ionic and electronic transport, interfacial compatibility, and electrochemical function. For Li-containing HEO-type compositions, lithium retention during spraying and post-treatment will also need to be assessed.

Thermal spray may not need to meet all SSTFB manufacturing requirements on its own to be useful. Its value may instead lie in enabling layer architectures and

thickness ranges that are difficult or inefficient to achieve by conventional thin-film routes, provided that the critical interfaces and electrolyte-quality requirements are addressed by suitable process combinations. The most realistic near- to mid-term route could be hybrid manufacturing. Thermal spray can provide rapid build-up, architectural flexibility, and compositional versatility, while complementary methods such as ALD, PVD, sputtering, laser treatment, sealant infiltration, or controlled-atmosphere processing can be used where interface precision, surface smoothing, defect reduction, or local densification are required.

Future progress should be staged around four priorities, as illustrated in Fig. 9. The first priority is reproducible deposition of individual battery-relevant layers, with different requirements for electrolytes, electrodes, current collectors, and interlayers. For electrolytes, ionic conductivity alone is not sufficient; density, electronic insulation, defect tolerance, controlled phase composition, and compatibility with adjacent layers are also important. For electrodes, the key requirements include controlled porosity, electronic and ionic transport, adhesion, mechanical integrity, and stable interfaces. For current collectors and conductive interlayers, electrical conductivity, chemical stability, adhesion, and interfacial compatibility are the main requirements. The second priority is better interface and defect control. Hybrid strategies such as VPS, laser treatment, sealant infiltration, and ALD or PVD interlayers may help address lithium/sodium loss, secondary phases, surface roughness, open porosity, and interfacial reactions. The third priority is the transition from isolated coatings towards multilayer and partial or full-cell stacks, where repeated thermal exposure, residual stress, roughness transfer, and interfacial resistance can be evaluated together. This is also where thermal spray may be combined with thin-film or post-treatment steps to produce more realistic hybrid multilayer architectures. The longer-term priority is controlled and traceable manufacturing. This includes pilot-scale processing, enclosed or partially enclosed spray cells, inline diagnostics, quality monitoring, and data-driven process control. Data-driven tools such as machine learning, digital twins, and closed-loop control based on real-time diagnostics could support this development by improving reproducibility and reducing trial-and-error process optimization (Ref 202-205). Used in this way, they can help translate thermal spray from promising battery-layer feasibility studies towards controlled and traceable SSTFB manufacturing.

Overall, thermal spray offers a promising but still developing scalable alternative processing route for selected SSTFB layers and hybrid architectures. Its strongest role is likely to be where high deposition rate, thickness flexibility, binder-free processing, or coating of larger-area and non-planar substrates provides a clear manufacturing advantage over conventional thin-film routes. This could become relevant for application-specific SSTFB designs where safety, form factor, lifetime, or integration matter as much as maximum energy density. Broader adoption will depend on whether sprayed battery layers can meet the microstructural, chemical, interfacial, contamination, and electrochemical requirements of complete devices. A balanced path forward is therefore not to present thermal spray as a universal replacement for conventional approaches to SSTFB fabrication, but to define where it adds manufacturing value and how it can be combined with established thin-film and post-treatment methods to produce reliable solid-state thin-film battery architectures.

Supplementary Information The online version contains supplementary material available at https://doi.org/10.1007/s11666-026-02327-x.

Acknowledgments This work was funded by the GREEN-BAT project (2022–2025) under the M-ERA.Net framework, with support from the Research Council of Finland, M-ERA.NET 3 (European Commission), and national/regional funders in Germany and Sweden. The Swedish part was additionally supported by the NovelCABs project (Swedish Energy Agency, Dnr 2021-002227) and Vinnova through M-ERA.NET 3. University of Turku also acknowledges the funding support from Tenure-Track grant to Prof. Ashish Ganvir; and Research Council of Finland for funding SOLACE, 360540 (2024-2028) project. Prof. Ashish Ganvir also acknowledges the Finnish Digital Design and Manufacturing Infrastructure (FiDiEm) for access to the experimental facilities.

Author Contributions AA contributed to visualization, formal analysis, and writing—original draft, review and editing; AH contributed to conceptualization, data curation, formal analysis, visualization, and writing—original draft; GV, NK and CN contributed to formal analysis and writing— original draft; AG contributed to conceptualization, funding acquisition, supervision, visualization, writing—original draft, review and editing; SJ contributed to conceptualization, funding acquisition, supervision, visualization, and writing—review and editing

Funding Open access funding provided by University West.

Declaration of Generative AI and AI Assisted Technologies in the Manuscript Preparation Process During the preparation of this work, the author(s) used ChatGPT in order to rephrase and grammar check author-written text. After using this tool/service, the author(s) reviewed and edited the content as needed and take(s) full responsibility for the content of the published article.

Open Access This article is licensed under a Creative Commons Attribution 4.0 International License, which permits use, sharing, adaptation, distribution and reproduction in any medium or format, as long as you give appropriate credit to the original author(s) and the source, provide a link to the Creative Commons licence, and indicate if changes were made. The images or other third party material in this article are included in the article's Creative Commons licence, unless indicated otherwise in a credit line to the material. If material is not included in the article's Creative Commons licence and your intended use is not permitted by statutory regulation or exceeds the permitted use, you will need to obtain permission directly from the copyright

holder. To view a copy of this licence, visit http://creativecommons.org/licenses/by/4.0/.

References

1. X. Feng, M. Ouyang, X. Liu, L. Lu, Y. Xia, and X. He, Thermal Runaway Mechanism of Lithium Ion Battery for Electric Vehicles: A Review, *Energy Storage Mater.*, 2018, **10**, p 246-267.
2. Y. Chen, Y. Kang, Y. Zhao, L. Wang, J. Liu, Y. Li, Z. Liang, X. He, X. Li, N. Tavajohi, and B. Li, A Review of Lithium-Ion Battery Safety Concerns: The Issues, Strategies, and Testing Standards, *J. Energy Chem.*, 2021, **59**, p 83-99.
3. X. Feng, D. Ren, X. He, and M. Ouyang, Mitigating Thermal Runaway of Lithium-Ion Batteries, *Joule*, 2020, **4**(4), p 743-770.
4. M. Armand and J.M. Tarascon, Building Better Batteries, *Nature*, 2008, **451**(7179), p 652-657.
5. A. Banerjee, X. Wang, C. Fang, E.A. Wu, and Y.S. Meng, Interfaces and Interphases in All-Solid-State Batteries with Inorganic Solid Electrolytes, *Chem. Rev.*, 2020, **120**(14), p 6878-6933.
6. Q. Xia, F. Zan, Q. Zhang, W. Liu, Q. Li, Y. He, J. Hua, J. Liu, J. Xu, J. Wang, C. Wu, and H. Xia, All-Solid-State Thin Film Lithium/Lithium-Ion Microbatteries for Powering the Internet of Things, *Adv. Mater.*, 2023, **35**(2), p 2200538.
7. P.H.L. Notten, F. Roozeboom, R.A.H. Niessen, and L. Baggetto, 3-D Integrated All-Solid-State Rechargeable Batteries, *Adv. Mater.*, 2007, **19**(24), p 4564-4567.
8. H. Ahmad, K.T. Kubra, A. Butt, U. Nisar, F.J. Iftikhar, and G. Ali, Recent Progress, Challenges, and Perspectives in the Development of Solid-State Electrolytes for Sodium Batteries, *J. Power. Sources*, 2023, **581**, p 233518.
9. M.H. Futscher, L. Brinkman, A. Müller, J. Casella, A. Aribia, and Y.E. Romanyuk, Monolithically-Stacked Thin-Film Solid-State Batteries, *Commun. Chem.*, 2023, **6**(1), p 110.
10. Y. Yu, M. Gong, C. Dong, and X. Xu, Thin-Film Deposition Techniques in Surface and Interface Engineering of Solid-State Lithium Batteries, *Next Nanotechnol.*, 2023, **3**(4), p 100028.
11. J. Janek and W.G. Zeier, A Solid Future for Battery Development, *Nat. Energy*, 2016 https://doi.org/10.1038/nenergy.2016.141
12. R. Karthikeyan, C.T. Cherian, and R.P. Fernandes, Review: RF Magnetron Sputtering, a Promising Synthesis Route for Scalable Production of Thin-Film Batteries, *J. Mater. Sci.*, 2025, **60**(21), p 8569-8601.
13. Y. Yao, X. Jiao, X. Xu, S. Xiong, Z. Song, and Y. Liu, Prospective of Magnetron Sputtering for Interface Design in Rechargeable Lithium Batteries, *Adv. Energy Mater.*, 2024, **14**(47), p 2403117.
14. G. Elomari, H. Larhlimi, R. Oubaki, E. Elmaataouy, M. Aqil, Y. Samih, M. Makha, C. Negrila, J. Alami, and M. Dahbi, Fast Charging and High-Efficiency Sputter-Deposited Silicon Thin Film Anodes for Li-Ion Batteries, *J. Power. Sources*, 2025, **642**, p 236967.
15. N. Kuwata, R. Kumar, K. Toribami, T. Suzuki, T. Hattori, and J. Kawamura, Thin Film Lithium Ion Batteries Prepared Only by Pulsed Laser Deposition, *Solid State Ionics*, 2006, **177**(26-32), p 2827-2832.
16. L. Indrizzi, N. Ohannessian, D. Pergolesi, T. Lippert, and E. Gilardi, Pulsed Laser Deposition as a Tool for the Development of All Solid-State Microbatteries, *Helv. Chim. Acta*, 2021, **104**(2), p e2000203.
17. M. Madadi, V. Miikkulainen, and M. Karppinen, Artificial Solid Electrolyte Interphases by Atomic and Molecular Layer Deposition, *Dalton Trans.*, 2025, **54**(27), p 10492-10503.
18. D. Go, J.W. Shin, S. Lee, J. Lee, B.C. Yang, Y. Won, M. Motoyama, and J. An, Atomic Layer Deposition for Thin Film Solid-State Battery and Capacitor, *Int. J. Precis. Eng. Manuf. Green Technol.*, 2023, **10**(3), p 851-873.
19. C. Wang, C. Wang, M. Li, S. Zhang, C. Zhang, S. Chou, J. Mao, and Z. Guo, Design of Thin Solid-State Electrolyte Films for Safe and Energy-Dense Batteries, *Mater. Today*, 2024, **72**, p 235-254.
20. J. Sung, J. Heo, D.-H. Kim, S. Jo, Y.-C. Ha, D. Kim, S. Ahn, and J.-W. Park, Recent Advances in All-Solid-State Batteries for Commercialization, *Mater. Chem. Front.*, 2024, **8**(8), p 1861-1887.
21. Y. Matsuda, N. Kuwata, and J. Kawamura, Thin-Film Lithium Batteries with 0.3-30 μm thick $LiCoO_2$ Films Fabricated by High-Rate Pulsed Laser Deposition, *Solid State Ionics*, 2018, **320**, p 38-44.
22. N.J. Dudney, Thin Film Micro-batteries, *Electrochem. Soc. Interface*, 2008, **17**(3), p 44.
23. M. Sahal, J. Molloy, V.R. Narayanan, L. Ladani, X. Lu, and N. Rolston, Robust and Manufacturable Lithium Lanthanum Titanate-Based Solid-State Electrolyte Thin Films Deposited in Open Air, *ACS Omega*, 2023, **8**(31), p 28651-28662.
24. S. Zhou, M. Li, P. Wang, L. Cheng, L. Chen, Y. Huang, S. Yu, F. Mo, and J. Wei, Printed Solid-State Batteries, *Electrochem. Energy Rev.*, 2023, **6**(1), p 34.
25. P. Vadhva, T.E. Gill, J.H. Cruddos, S. Said, M. Siniscalchi, S. Narayanan, M. Pasta, T.S. Miller, and A.J.E. Rettie, Engineering Solution-Processed Non-crystalline Solid Electrolytes for Li Metal Batteries, *Chem. Mater.*, 2023, **35**(3), p 1168-1176.
26. J. Minkiewicz, G.M. Jones, S. Ghanizadeh, S. Bostanchi, T.J. Wasely, S.A. Yamini, and V. Nekouie, Large-Scale Manufacturing of Solid-State Electrolytes: Challenges, Progress, and Prospects, *Open Ceram.*, 2023, **16**, p 100497.
27. L. Pawlowski, *The Science and Engineering of Thermal Spray Coatings*, John Wiley & Sons, 2008.
28. S. Joshi and P. Nylen, Advanced Coatings by Thermal Spray Processes, *Technologies*, 2019, **7**(4), p 79.
29. A. Hasani, S. Joshi, A. Salminen, S. Goel, J. Reuteler, M.G. Makowska, and A. Ganvir, Localized Phase and Elemental Mapping in Solid-State Lithium Battery LTO Anode Thin-Film Produced by a Novel Suspension Plasma Spray Approach, *J. Therm. Spray Technol.*, 2025, **34**(5), p 1589-1597.
30. A. Hasani, Characterization of thermally sprayed thin-film all-solid-state batteries, PhD thesis, retrieved from. https://urn.fi/URN:ISBN:978-952-02-0546-1
31. V. Gopal, K. Clovis, S. Björklund, A. Balapure, S. Goel, A. Hall, R. Younesi, and S. Joshi, Exploring Atmospheric Plasma Spraying as a Pathway to Fabricate Solid-State Battery Constituents, *Surf. Coat. Technol.*, 2025, **502**, p 131945.
32. A. Hasani, S. Joshi, A. Salminen, S. Goel, A. Breard, M. Juan, M.G. Makowska, E. Mäkilä, C. Nayak, and A. Ganvir, Advanced synchrotron micro characterization of laser post-processed plasma sprayed LLZO solid-state battery electrolyte, IOP Conference Series: Materials Science and Engineering, IOP Publishing, 012022 2025
33. X.-B. Cheng, C.-Z. Zhao, Y.-X. Yao, H. Liu, and Q. Zhang, Recent Advances in Energy Chemistry Between Solid-State Electrolyte and Safe Lithium-Metal Anodes, *Chem*, 2019, **5**(1), p 74-96.
34. J. Bates, N. Dudney, B. Neudecker, A. Ueda, and C. Evans, Thin-Film Lithium and Lithium-Ion Batteries, *Solid State Ionics*, 2000, **135**(1-4), p 33-45.

35. D.L. Nelson, S.E. Sandoval, J. Pyo, D. Bistri, T.A. Thomas, K.A. Cavallaro, J.A. Lewis, A.S. Iyer, P. Shevchenko, and C.V. Di Leo, Fracture Dynamics in Silicon Anode Solid-State Batteries, *ACS Energy Lett.*, 2024, **9**(12), p 6085-6095.
36. B. Wu, C. Chen, D.L. Danilov, R.-A. Eichel, and P.H.L. Notten, All-Solid-State Thin Film Li-Ion Batteries: New Challenges, New Materials, and New Designs, *Batteries*, 2023, **9**(3), p 186.
37. A. Pearse, T. Schmitt, E. Sahadeo, D.M. Stewart, A. Kozen, K. Gerasopoulos, A.A. Talin, S.B. Lee, G.W. Rubloff, and K.E. Gregorczyk, Three-Dimensional Solid-State Lithium-Ion Batteries Fabricated by Conformal Vapor-Phase Chemistry, *ACS Nano*, 2018, **12**(5), p 4286-4294.
38. S. Nowak, F. Berkemeier, and G. Schmitz, Ultra-thin LiPON Films – Fundamental Properties and Application in Solid State Thin Film Model Batteries, *J. Power. Sources*, 2015, **275**, p 144-150.
39. C. Glynn and C. O'Dwyer, Solution Processable Metal Oxide Thin Film Deposition and Material Growth for Electronic and Photonic Devices, *Adv. Mater. Interfaces*, 2017, **4**(2), p 1600610.
40. P. Molaiyan, J. Valikangas, R. Sliz, D. Ramteke, T. Hu, A. Paolella, T. Fabritius, and U. Lassi, Screen-Printed Composite $LiFePO_4$-LLZO Cathodes Towards Solid-State Li-Ion Batteries, *ChemElectroChem*, 2024, **11**(9), p e202400051.
41. G. Vanheusden, L.L. De Taeye, R.M. López-Báez, A.I.P. Martinez, and P.M. Vereecken, Electrochemically Induced Sol-Gel Deposition of Solid Electrolyte Thin Films for Li-Ion Batteries, *J. Electrochem. Soc.*, 2025, **172**(9), p 092506.
42. L. Klein, M. Aparicio, and F. Damay, Sol-Gel Processing for Battery and Fuel Cell Applications. Handbook of Sol-Gel Science and Technology: Processing, Characterization and applications, p 311 2005
43. S. Kim, H. Lee, J. Park, M. Ku, M. Kim, and Y.-B. Kim, Lithium-Preserved Sintering Method for Perovskite-Based Solid Electrolyte Thin Films via Flash Light Sintering for All-Solid-State Lithium-Ion Batteries, *J. Mater. Chem. A*, 2023, **11**(40), p 21586-21594.
44. S. Uhlenbruck, J. Dornseiffer, S. Lobe, C. Dellen, C.-L. Tsai, B. Gotzen, D. Sebold, M. Finsterbusch, and O. Guillon, Cathode-Electrolyte Material Interactions during Manufacturing of Inorganic Solid-State Lithium Batteries, *J. Electroceram.*, 2017, **38**(2), p 197-206.
45. W. Xu, J. Wang, F. Ding, X. Chen, E. Nasybulin, Y. Zhang, and J.-G. Zhang, Lithium Metal Anodes for Rechargeable Batteries, *Energy Environ. Sci.*, 2014, **7**(2), p 513-537.
46. I. Madinabeitia, J. Rikarte, A. Etxebarria, G. Baraldi, F.J. Fernández-Carretero, I. Garbayo, R. Cid, A. García-Luis, and M.Á. Muñoz-Márquez, Monolithic All-Solid-State High-Voltage Li-Metal Thin-Film Rechargeable Battery, *ACS Appl. Energy Mater.*, 2022, **5**(10), p 12120-12131.
47. A.S. Westover, R. Sahore, K.L. Browning, and S. Kalnaus, Thermal Evaporation of Thin Li Films, *J. Vac. Sci. Technol. B*, 2025 https://doi.org/10.1116/6.0004174
48. A.J. Lovett, A. Kursumovic, and J.L. MacManus-Driscoll, Lithium Loss in Vacuum Deposited Thin Films, *ACS Energy Lett.*, 2024, **9**(4), p 1753-1758.
49. K. Schönherr, M. Pöthe, B. Schumm, H. Althues, C. Leyens, and S. Kaskel, Tailored Pre-lithiation Using Melt-Deposited Lithium Thin Films, *Batteries*, 2023, **9**(1), p 53.
50. M. Liu, A. Song, X. Zhang, J. Wang, Y. Fan, G. Wang, H. Tian, Z. Ma, and G. Shao, Interfacial Lithium-Ion Transportation in Solid-State Batteries: Challenges and Prospects, *Nano Energy*, 2025, **136**, p 110749.
51. A. Machín, F. Díaz, M.C. Cotto, J. Ducongé, and F. Márquez, Recent Advances in Dendrite Suppression Strategies for Solid-State Lithium Batteries: From Interface Engineering to Material Innovations, *Batteries*, 2025, **11**(8), p 304.
52. Y. Mao, T. Wang, F. Yin, and C. Sun, In Situ Formation of Li3N Interlayer Enhancing Interfacial Stability of Solid-State Lithium Batteries, *J. Colloid Interface Sci.*, 2025, **685**, p 595-603.
53. W. Jia, J. Zhang, L. Zheng, H. Zhou, W. Zou, and L. Wang, Lithium-Rich Alloy as Stable Lithium Metal Composite Anode for Lithium Batteries, *Escience*, 2024, **4**(6), p 100266.
54. J. Aspinall, Y. Chart, H. Guo, P. Shrestha, M. Burton, and M. Pasta, Effect of Microstructure on the Cycling Behavior of Li-In Alloy Anodes for Solid-State Batteries, *ACS Energy Lett.*, 2024, **9**(2), p 578-585.
55. Z. Wu, X. Xiong, R. Xu, Y. Ma, X.-B. Cheng, Z. Zhu, L. Liu, S. Peng, T. Wang, and Y. Wu, Lithium Alloy Anodes for All-Solid-State Lithium Batteries: From Failure Mechanism to Performance-Oriented Design, *J. Mater. Chem. A*, 2025, **13**(41), p 35054-35081.
56. H. Huo and J.R. Janek, Silicon as Emerging Anode in Solid-State Batteries, *ACS Energy Lett.*, 2022, **7**(11), p 4005-4016.
57. M. Haro, P. Kumar, J. Zhao, P. Koutsogiannis, A.J. Porkovich, Z. Ziadi, T. Bouloumis, V. Singh, E.J. Juarez-Perez, and E. Toulkeridou, Nano-vault Architecture Mitigates Stress in Silicon-Based Anodes for Lithium-Ion Batteries, *Commun. Mater.*, 2021, **2**(1), p 16.
58. J. Sakabe, N. Ohta, T. Ohnishi, K. Mitsuishi, and K. Takada, Porous Amorphous Silicon Film Anodes for High-Capacity and Stable All-Solid-State Lithium Batteries, *Commun. Chem.*, 2018, **1**(1), p 24.
59. H. Pan, L. Wang, Y. Shi, C. Sheng, S. Yang, P. He, and H. Zhou, A Solid-State Lithium-Ion Battery with Micron-Sized Silicon Anode Operating Free From External Pressure, *Nat. Commun.*, 2024, **15**(1), p 2263.
60. Y. Suh, J.K. Koo, H.-j Im, and Y.-J. Kim, Astonishing Performance Improvements of Dry-Film Graphite Anode for Reliable Lithium-Ion Batteries, *Chem. Eng. J.*, 2023, **476**, p 146299.
61. S. Fang, D. Bresser, and S. Passerini, Transition metal oxide anodes for electrochemical energy storage in lithium-and sodium-ion batteries, *Transition Metal Oxides for Electrochemical Energy Storage*. 2022, p 55-99
62. S. Lhagvajav, E. Enkhbayar, S. Galsan, and A. Pagvajav, $Li_4Ti_5O_{12}$/Graphene composite as an anode for Li-ion battery, *Scientific transaction of the National University of Mongolia. Physics*, 2019, 29(518), p 80-83
63. W. Duan, S. Chen, X. Zhuang, N. Jiang, and Y. Li, Anode Materials for Sodium-Ion Batteries: Current Status and Future Perspectives, *J. Power. Sources*, 2026, **666**, p 239163.
64. A.U. Rehman, S. Saleem, S. Ali, S.M. Abbas, M. Choi, and W. Choi, Recent Advances in Alloying Anode Materials for Sodium-Ion Batteries: Material Design and Prospects, Energy Mater., 4(6) (2024)
65. Z. Qi and H. Wang, Advanced Thin Film Cathodes for Lithium Ion Batteries, *Research*, 2020 https://doi.org/10.34133/2020/2969510
66. R. Deokate and P. Barpanda, High-Stability Cathode Materials for Sodium-Ion Batteries: Optimization Strategies and Promising Future Applications, *J. Mater. Chem. A*, 2026, **14**(12), p 6749-6771.
67. G. Sun, Y. Ma, H. Zhang, S. Wu, S. Chu, S. Passerini, and Y. Ma, Fabrication of Composite Cathode for All-Solid-State Sodium Batteries, *Adv. Energy Mater.*, 2025 https://doi.org/10.1002/aenm.202503756
68. Z. Duan, Y. Wu, J. Lin, L. Wang, and D.-L. Peng, Thin-Film Lithium Cobalt Oxide for Lithium-Ion Batteries, *Energies*, 2022, **15**(23), p 8980.

69. C.M. Julien, A. Mauger, and O.M. Hussain, Sputtered $LiCoO_2$ Cathode Materials for All-Solid-State Thin-Film Lithium Microbatteries, *Materials*, 2019, **12**(17), p 2687.
70. Z. Benzarti, J.D. Castro, E. Carneiro, L. Pacheco, N. Duarte, S. Carvalho, R. Serra, A. Cavaleiro, C. Alves, and S. Cruz, Effect of Annealing on $LiCoO_2$ Thin Film Deposited by RF Magnetron Sputtering, *Materials*, 2025, **18**(6), p 1217.
71. B. Jaklič, J. Žuntar, E. Tchernychova, G. Kapun, M. Šala, R. Dominko, and M. Spreitzer, Structural Changes and Mechanisms of Reversible Electrochemical Lithium-Ion Cycling in (104) Oriented $LiNi_{1/3}Mn_{1/3}Co_{1/3}O_2$ Thin Film Cathodes Prepared by Pulsed Laser Deposition, *RSC Adv.*, 2025, **15**(14), p 10787-10800.
72. M. Hallot, B. Caja-Munoz, C. Leviel, O.I. Lebedev, R. Retoux, J. Avila, P. Roussel, M.C. Asensio, and C. Lethien, Atomic Layer Deposition of a Nanometer-thick Li3PO4 Protective Layer on LiNi0.5Mn1.5O4 Films: Dream or Reality for Long-Term Cycling?, *ACS Appl. Mater. Interfaces*, 2021, **13**(13), p 15761-15773.
73. L. Wang, L.-C. Zhang, I. Lieberwirth, H.-W. Xu, and C.-H. Chen, A $Li_3V_2(PO_4)_3$/C Thin Film with High Rate Capability as a Cathode Material for Lithium-Ion Batteries, *Electrochem. Commun.*, 2010, **12**(1), p 52-55.
74. V. Siller, J.C. Gonzalez-Rosillo, M.N. Eroles, F. Baiutti, M.O. Liedke, M. Butterling, A.G. Attallah, E. Hirschmann, A. Wagner, and A. Morata, Nanoscaled LiMn2O4 for Extended Cycling Stability in the 3 V Plateau, *ACS Appl. Mater. Interfaces*, 2022, **14**(29), p 33438-33446.
75. B. Uzakbaiuly, A. Mukanova, Y. Zhang, and Z. Bakenov, Physical Vapor Deposition of Cathode Materials for All Solid-State Li Ion Batteries: A Review, *Front. Energy Res.*, 2021, **9**, p 625123.
76. A.A. Pavlovskii, K. Pushnitsa, A. Kosenko, P. Novikov, and A.A. Popovich, 3D-Printed Lithium-Ion Battery Electrodes: A Brief Review of Three Key Fabrication Techniques, *Materials*, 2024, **17**(23), p 5904.
77. D. Ren, L. Lu, R. Hua, G. Zhu, X. Liu, Y. Mao, X. Rui, S. Wang, B. Zhao, and H. Cui, Challenges and Opportunities of Practical Sulfide-Based All-Solid-State Batteries, *Etransportation*, 2023, **18**, p 100272.
78. T. Brahmbhatt, G. Yang, E.C. Self, and J. Nanda, Cathode–Sulfide Solid Electrolyte Interfacial Instability: Challenges and Solutions, *Front. Energy Res.*, 2020, **8**, p 570754.
79. C. Ye, S. Xu, H. Li, J. Shan, and S.Z. Qiao, Developing Cathode Films for Practical All-Solid-State Lithium-Sulfur Batteries, *Adv. Mater.*, 2025, **37**(23), p 2407738.
80. A.C. Kozen, A.J. Pearse, C.-F. Lin, M. Noked, and G.W. Rubloff, Atomic Layer Deposition of the Solid Electrolyte LiPON, *Chem. Mater.*, 2015, **27**(15), p 5324-5331.
81. B. Put, P.M. Vereecken, J. Meersschaut, A. Sepúlveda, and A. Stesmans, Electrical Characterization of Ultrathin RF-Sputtered LiPON Layers for Nanoscale Batteries, *ACS Appl. Mater. Interfaces*, 2016, **8**(11), p 7060-7069.
82. W. Berthou, M. Legallais, S. Sorieul, G. Yildirim, B. Bousquet, V. Motto-Ros, and F. Le Cras, High-Throughput Experimentation Unveils Composition–Structure–Conductivity Relationships in the Extended LiPON System, *Adv. Energy Mater.*, 2024, **14**(36), p 2400656.
83. J. Ko and Y.S. Yoon, Influence of Process Conditions on Structural and Electrochemical Properties of Lithium Phosphorus Oxynitride Thin Films, *Ceram. Int.*, 2020, **46**(13), p 20623-20632.
84. J.P. Singh, A.K. Paidi, and S. Lee, Growth Strategies of $Li_{7-}La_3Zr_2O_{12}$ Electrolytes for Li-Ion Thin Film Battery, *Chem. Eng. J. Adv.*, 2023, **16**, p 100532.
85. G.B. Crane, T.W. Colburn, S.E. Holmes, J. Just, Y. Cui, and R.H. Dauskardt, Rapid Scalable Plasma Processing of Thin-Film Li-La-Zr-O Solid-State Electrolytes, *Matter*, 2025 https://doi.org/10.1016/j.matt.2025.102468
86. E. Kazyak, K.-H. Chen, K.N. Wood, A.L. Davis, T. Thompson, A.R. Bielinski, A.J. Sanchez, X. Wang, C. Wang, and J. Sakamoto, Atomic Layer Deposition of the Solid Electrolyte Garnet $Li_7La_3Zr_2O_{12}$, *Chem. Mater.*, 2017, **29**(8), p 3785-3792.
87. P.W. Jaschin, C.R. Tang, and E.D. Wachsman, Fast Charging and Low Temperature Capabilities of Sodium Solid-State Batteries Enabled by Thin NASICON Bilayer Architecture, *ACS Energy Lett.*, 2025, **10**(6), p 2610-2616.
88. Y. Dong, P. Wen, H. Shi, Y. Yu, and Z.S. Wu, Solid-State Electrolytes for Sodium Metal Batteries: Recent Status and Future Opportunities, *Adv. Funct. Mater.*, 2024, **34**(5), p 2213584.
89. H. Su, Z. Jiang, Y. Liu, J. Li, C. Gu, X. Wang, X. Xia, and J. Tu, Recent Progress of Sulfide Electrolytes for All-Solid-State Lithium Batteries, Energy Mater., 2(1) (2022)
90. B. Man, Y. Zeng, Q. Liu, Y. Chen, X. Li, W. Luo, Z. Zhang, C. He, M. Jie, and S. Liu, A Comprehensive Review of Sulfide Solid-State Electrolytes: Properties, Synthesis, Applications, and Challenges, *Crystals*, 2025, **15**(6), p 492.
91. J. Xu, L. Liu, N. Yao, F. Wu, H. Li, and L. Chen, Liquid-Involved Synthesis and Processing of Sulfide-Based Solid Electrolytes, Electrodes, and All-Solid-State Batteries, *Mater. Today Nano*, 2019, **8**, p 100048.
92. X. Guo, S. Halacoglu, Y. Chen, and H. Wang, Recent Progress on Dominant Sulfide-Type Solid-State Na Superionic Conductors for Solid-State Sodium Batteries, *Small*, 2024, **20**(33), p 2311195.
93. L.P. Teo, M.H. Buraidah, and A.K. Arof, Development on Solid Polymer Electrolytes for Electrochemical Devices, *Molecules*, 2021, **26**(21), p 6499.
94. F. Gucci, M. Grasso, C. Shaw, G. Leighton, V.M. Rodriguez, and J. Brighton, PEO-Based Polymer Blend Electrolyte for Composite Structural Battery, *Polym. -Plast. Technol. Mater.*, 2023, **62**(8), p 1019-1028.
95. Z. Yao, F. Qi, L. Ye, Q. Sun, X. Gu, X. Yang, and K. Zhu, Composite Polymer Electrolyte Based on Poly (vinylidene Fluoride-Hexafluoropropylene)(PVDF-HFP) for Solid-State Batteries, *Heliyon*, 2024 https://doi.org/10.1016/j.heliyon.2024.e28097
96. S.-Y. Du, G.-X. Ren, N. Zhang, and X.-S. Liu, High-Performance Poly (Vinylidene Fluoride-Hexafluoropropylene)-Based Composite Electrolytes with Excellent Interfacial Compatibility for Room-Temperature All-Solid-State Lithium Metal Batteries, *ACS Omega*, 2022, **7**(23), p 19631-19639.
97. C.-Y. Wu, Q. Bao, Y.C. Lai, X. Liu, Y.-C. Lu, H. Tao, and J.-G. Duh, In-Situ Thermal Annealing Pt/Ti Interphase Layers for Epitaxial Growth of Improved Li $(Ni_{0.5}Mn_{0.3}Co_{0.2})$ O_2 Solid Thin-Film Cathodes, *Nano Energy*, 2019, **60**, p 784-793.
98. A. Müller, L. Paravicini, J. Morzy, M. Krause, J. Casella, N. Osenciat, M.H. Futscher, and Y.E. Romanyuk, Influence of Au, Pt, and C Seed Layers on Lithium Nucleation Dynamics for Anode-Free Solid-State Batteries, *ACS Appl. Mater. Interfaces*, 2023, **16**(1), p 695-703.
99. S. Lobe, A. Bauer, S. Uhlenbruck, and D. Fattakhova-Rohlfing, Physical Vapor Deposition in Solid-State Battery Development: From Materials to Devices, *Adv. Sci.*, 2021, **8**(11), p 2002044.
100. M. Ihrig, M. Finsterbusch, A.M. Laptev, C.-H. Tu, N.T.T. Tran, C.-A. Lin, L.-Y. Kuo, R. Ye, Y.J. Sohn, and P. Kaghazchi, Study of LiCoO2/Li7La3Zr2O12: Ta Interface Degradation in All-Solid-State Lithium Batteries, *ACS Appl. Mater. Interfaces*, 2022, **14**(9), p 11288-11299.

101. S. Liang, D. Yang, J. Hu, S. Kang, X. Zhang, and Y. Fan, $Li_7La_3Zr_2O_{12}$-co-$LiNbO_3$ Surface Modification Improves the Interface Stability Between Cathode and Sulfide Solid-State Electrolyte in All-Solid-State Batteries, *Membranes*, 2023, **13**(2), p 216.
102. M.M. Mashfy, T.A. Alvy, N. Hossain, M.A. Haque, F.T. Mohsin, T. Sharmin, and M. Nasim, Sodium Ion Batteries: A Sustainable Alternative to Lithium-Ion Batteries with an Overview of Market Trends, Recycling, and Battery Chemistry, *Next Energy*, 2026, **10**, p 100478.
103. H. Aziam, B. Larhrib, C. Hakim, N. Sabi, H.B. Youcef, and I. Saadoune, Solid-State Electrolytes for Beyond Lithium-Ion Batteries: A Review, *Renew. Sustain. Energy Rev.*, 2022, **167**, p 112694.
104. S. Lee, S. Kim, Y.-R. Jo, B. Im, D.G. Kim, J.-Y. Jeon, S. Yang, and G.-H. An, Interface-Engineered Current Collectors for Improved Rate Performance in Solid-State Lithium-Ion Batteries, *J. Alloys Compd.*, 2025, **1036**, p 181961.
105. X. Liu, R. Garcia-Mendez, A.R. Lupini, Y. Cheng, Z.D. Hood, F. Han, A. Sharafi, J.C. Idrobo, N.J. Dudney, and C. Wang, Local Electronic Structure Variation Resulting in Li 'Filament'formation Within Solid Electrolytes, *Nat. Mater.*, 2021, **20**(11), p 1485-1490.
106. L.-P. Wang, X.-D. Zhang, T.-S. Wang, Y.-X. Yin, J.-L. Shi, C.-R. Wang, and Y.-G. Guo, Ameliorating the Interfacial Problems of Cathode and Solid-State Electrolytes by Interface Modification of Functional Polymers, *Adv. Energy Mater.*, 2018, **8**(24), p 1801528.
107. H. Huo, Y. Bai, S.L. Benz, T. Weintraut, S. Wang, A. Henss, D. Raabe, and J. Janek, Decoupling the Effects of Interface Chemical Degradation and Mechanical Cracking in Solid-State Batteries with Silicon Electrode, *Adv. Mater.*, 2025, **37**(7), p 2415006.
108. J.H. Woo, J.E. Trevey, A.S. Cavanagh, Y.S. Choi, S.C. Kim, S.M. George, K.H. Oh, and S.-H. Lee, Nanoscale Interface Modification of $LiCoO_2$ by Al_2O_3 Atomic Layer Deposition for Solid-State Li Batteries, *J. Electrochem. Soc.*, 2012, **159**(7), p A1120-A1124.
109. Y.-W. Byeon and H. Kim, Review on Interface and Interphase Issues in Sulfide Solid-State Electrolytes for All-Solid-State Li-Metal Batteries, *Electrochem*, 2021, **2**(3), p 452-471.
110. S. Luo, Z. Wang, X. Li, X. Liu, H. Wang, W. Ma, L. Zhang, L. Zhu, and X. Zhang, Growth of Lithium-Indium Dendrites in All-Solid-State Lithium-Based Batteries with Sulfide Electrolytes, *Nat. Commun.*, 2021, **12**(1), p 6968.
111. J.H. Woo, J.J. Travis, S.M. George, and S.-H. Lee, Utilization of Al_2O_3 Atomic Layer Deposition for Li Ion Pathways in Solid State Li Batteries, *J. Electrochem. Soc.*, 2015, **162**(3), p A344-A349.
112. J. Su, M. Pasta, Z. Ning, X. Gao, P.G. Bruce, and C.R. Grovenor, Interfacial Modification Between Argyrodite-Type Solid-State Electrolytes and Li Metal Anodes Using LiPON Interlayers, *Energy Environ. Sci.*, 2022, **15**(9), p 3805-3814.
113. A.S. Westover, N.J. Dudney, R.L. Sacci, and S. Kalnaus, Deposition and Confinement of Li Metal Along an Artificial LiPON–LiPON Interface, *ACS Energy Lett.*, 2019, **4**(3), p 651-655.
114. Y. Hamon, A. Douard, F. Sabary, C. Marcel, P. Vinatier, B. Pecquenard, and A. Levasseur, Influence of Sputtering Conditions on Ionic Conductivity of LiPON Thin Films, *Solid State Ionics*, 2006, **177**(3-4), p 257-261.
115. R. Thirupathi, R.P. Srivastava, B. Patankar, S. Bhattacharyya, M. Aman, S. Sharma, and S. Omar, Advancing NASICON-Structured Solid-State Sodium-Ion Batteries through Compositional and Interfacial Engineering, *Chem. Commun. (Camb.)*, 2025, **61**(59), p 10931-10951.
116. N.J. Dudney, Solid-State Thin-Film Rechargeable Batteries, *Mater. Sci. Eng. B*, 2005, **116**(3), p 245-249.
117. M. Curcio, R. Teghil, and A. De Bonis, Thin-Film Microbattery Fabrication by PLD: A Comprehensive Mini-review, *Front. Coat. Dyes Interface Eng.*, 2024, **2**, p 1401391.
118. L. Han, C.-T. Hsieh, B.C. Mallick, J. Li, and Y.A. Gandomi, Recent Progress and Future Prospects of Atomic Layer Deposition to Prepare/Modify Solid-State Electrolytes and Interfaces Between Electrodes for Next-Generation Lithium Batteries, *Nanoscale Adv.*, 2021, **3**(10), p 2728-2740.
119. A.S.M. Ang and C.C. Berndt, A Review of Testing Methods for Thermal Spray Coatings, *Int. Mater. Rev.*, 2014, **59**(4), p 179-223.
120. T. Hervy, N. Curry, S. Björklund, F. Lukac, and S. Joshi, Axial Plasma Spraying of Aqueous Solution Precursors: A Facile Approach for Columnar Thermal Barrier Coatings, *J. Eur. Ceram. Soc.*, 2025, **45**(6), p 117189.
121. A. Pasupathi, P. Kandasamy, R.K. Dharman, S. Govindarajan, T.H. Oh, M.W. Lee, and Y. Subramaniam, A Facile Approach to Deposit High Performance Electrocatalyst High Entropy Oxide Coatings Using a Novel Plasma Spray Route for Efficient Water Splitting in an Alkaline Medium, *Sustain. Energy Fuels*, 2025, **9**(12), p 3323-3334.
122. G. Vinay, S. Björklund, I. Angervo, A. Ganvir, and S. Joshi, Scalable Single-Step Fabrication of High-Entropy Oxide Coatings by Axial Solution Precursor Plasma Spray, *J. Eur. Ceram. Soc.*, 2026, **46**(8), p 118150.
123. L. Xie, X. Ma, E.H. Jordan, N.P. Padture, D.T. Xiao, and M. Gell, Deposition of Thermal Barrier Coatings Using the Solution Precursor Plasma Spray Process, *J. Mater. Sci.*, 2004, **39**(5), p 1639-1646.
124. S. Mathiyalagan, S. Björklund, S.J. Storm, G. Salian, R. Le Ruyet, R. Younesi, and S. Joshi, Facile One-Step Fabrication of $Li_4Ti_5O_{12}$ Coatings by Suspension Plasma Spraying, *Mater. Res. Bull.*, 2025, **181**, p 113111.
125. V.S. Rangasamy and A. Vanhulsel, Synthesis and Processing of Battery Materials: Giving it the Plasma Touch, *Batteries Supercaps*, 2021, **4**(5), p 692-716.
126. D. Soysal, J. Arnold, P. Szabo, R. Henne, and S.A. Ansar, Thermal Plasma Spraying Applied on Solid Oxide Fuel Cells, *J. Therm. Spray Technol.*, 2013, **22**(5), p 588-598.
127. M. Jadidi, S. Moghtadernejad, and A. Dolatabadi, A Comprehensive Review on Fluid Dynamics and Transport of Suspension/Liquid Droplets and Particles in High-Velocity Oxygen-Fuel (HVOF) Thermal Spray, *Coatings*, 2015, **5**(4), p 576-645.
128. J. Yu, X. Liu, Y. Yu, Z. Li, S. Xu, H. Li, P. Liu, and L. Wang, Effect of HVOF Spraying Process on Particle Behavior of Fe-Based Amorphous Alloy Coatings, *J. Therm. Spray Technol.*, 2022, **31**(8), p 2448-2462.
129. H. Assadi, H. Kreye, F. Gärtner, and T. Klassen, Cold Spraying–a Materials Perspective, *Acta Mater.*, 2016, **116**, p 382-407.
130. D. Hanft, J. Exner, M. Schubert, T. Stöcker, P. Fuierer, and R. Moos, An Overview of the Aerosol Deposition Method: Process Fundamentals and New Trends in Materials Applications, *J. Ceram. Sci. Technol.*, 2015, **6**(3), p 147-182.
131. Z. Yu, B. Wang, L. Gui, M. Liu, S. Liu, M. Moliere, and H. Liao, Development of Photocatalytic and Electrocatalytic Coatings via Thermal Spraying for Environmental and Energy Storage Applications: A Short Review, *Surf. Sci. Technol.*, 2024, **2**(1), p 7.
132. B. Neudecker, N. Dudney, and J. Bates, "Lithium-Free" Thin-Film Battery with In Situ Plated Li Anode, *J. Electrochem. Soc.*, 2000, **147**(2), p 517-523.
133. X. Gao, L. Jia, and X. Zhang, Interface Engineering for Silicon/Carbon Composite Anode in All-Solid-State Batteries, *Energy Mater. Devices*, 2025, **3**(3), p 9370067.

134. F. Liang, L. Yang, R. Hu, B. Yuan, M. Zhu, and J. Liu, Mechanisms, Development, and Applications of Silicon-Based Anodes in Solid State Batteries, *Chem. Sci.*, 2026, **17**(2), p 738-771.
135. D. Yost, J. Laurer, K. Childrey, C. Cai, and G.M. Koenig, Fabrication and Characterization of Plasma Sprayed TiO_2 and Li4Ti5O12 Materials as All Active Material Lithium-Ion Battery Electrodes, *Batteries*, 2023, **9**(12), p 598.
136. L. Gopal and T. Sudarshan, Plasma-Driven Strategies for Advanced Composite Coatings, *Surf. Eng.*, 2026, **42**(4), p 369-377.
137. S. Huo, L. Sheng, W. Xue, L. Wang, H. Xu, H. Zhang, B. Su, M. Lyu, and X. He, Challenges of Stable ion Pathways in Cathode Electrode for All-Solid-State Lithium Batteries: A Review, *Adv. Energy Mater.*, 2023, **13**(15), p 2204343.
138. C. Lee, S. Kim, and J.S. Kang, Spinel-Structured Nickel Manganese Oxides for Electrochemical Magnesium Recovery, *ACS Electrochem.*, 2026, **2**(4), p 922-930.
139. Z. Wang, J. Yuan, X. Zhu, H. Wang, L. Huang, Y. Wang, and S. Xu, Overcharge-to-Thermal-Runaway Behavior and Safety Assessment of Commercial Lithium-Ion Cells with Different Cathode Materials: A Comparison Study, *J. Energy Chem.*, 2021, **55**, p 484-498.
140. H. Li, X. Xiao, J. Wu, X. Wu, R. Chen, Y. Cao, X. Ai, and Z. Chen, Progress of LiMnyFe1−yPO_4 Cathode Materials: From Mechanisms, Defects, Modification Methods to Applications, *Carbon Neutralization*, 2025, **4**(3), p e70009.
141. Y. Wu, K. Wang, K. Liu, Y. Long, C. Yang, H. Zhang, W. Pan, W. Si, and H. Wu, Rapid Processing of Uniform, Thin, Robust, and Large-Area Garnet Solid Electrolyte by Atmospheric Plasma Spraying, *Adv. Energy Mater.*, 2023, **13**(30), p 2300809.
142. B. Wang, Y. Zhao, M.N. Banis, Q. Sun, K.R. Adair, R. Li, T.-K. Sham, and X. Sun, Atomic Layer Deposition of Lithium Niobium Oxides as Potential Solid-State Electrolytes for Lithium-Ion Batteries, *ACS Appl. Mater. Interfaces*, 2018, **10**(2), p 1654-1661.
143. T. Lee, J. Qi, C.A. Gadre, H. Huyan, S.-T. Ko, Y. Zuo, C. Du, J. Li, T. Aoki, R. Wu, J. Luo, S.P. Ong, and X. Pan, Atomic-Scale Origin of the Low Grain-Boundary Resistance in Perovskite Solid Electrolyte Li0.375Sr0.4375Ta0.75Zr0.25O3, *Nat. Commun.*, 2023, **14**(1), p 1940.
144. X.-C. Bu, N. Chen, X.-T. Luo, and C.-J. Li, Plasma Spray Deposition of Na3Zr2Si2PO12 Electrolyte for High-Performance All-Solid-State Sodium-Ion Battery, *J. Therm. Spray Technol.*, 2025, **34**(2), p 495-505.
145. G. Kumar Mishra, M. Gautam, K. Bhawana, C. Sah Kalwar, M. Patro, Anshu, and S. Mitra, Exploring Chemical and Electrochemical Limitations in Sulfide Solid State Electrolytes: A Critical Review on Current Status and Manufacturing Scope, *Chem. Eur. J.*, 2024, **30**(71), p e202402510.
146. C.-J. Li, X.-T. Luo, S.-W. Yao, G.-R. Li, C.-X. Li, and G.-J. Yang, The Bonding Formation during Thermal Spraying of Ceramic Coatings: A Review, *J. Therm. Spray Technol.*, 2022, **31**(4), p 780-817.
147. R. Trócoli, A. Dushina, S. Borhani-Haghighi, A. Ludwig, and F. La Mantia, Effect of Pt and Au Current Collector in $LiMn2O_4$ Thin Film for Micro-batteries, *Nanotechnology*, 2018, **29**(3), p 035404.
148. M. Yamada, T. Watanabe, T. Gunji, J. Wu, and F. Matsumoto, Review of the Design of Current Collectors for Improving the Battery Performance in Lithium-Ion and Post-lithium-ion Batteries, *Electrochem.*, 2020, **1**(2), p 124-159.
149. A. Moridi, S.M. Hassani-Gangaraj, M. Guagliano, and M. Dao, Cold Spray Coating: Review of Material Systems and Future Perspectives, *Surf. Eng.*, 2014, **30**(6), p 369-395.
150. D. Tejero-Martin, M. Rezvani Rad, A. McDonald, and T. Hussain, Beyond Traditional Coatings: A Review on Thermal-Sprayed Functional and Smart Coatings, *J. Therm. Spray Technol.*, 2019, **28**(4), p 598-644.
151. J. Wilden and A. Wank, Production of Superplastic Foils by Thermal Spraying, *Proceedings of the ITSC*, 2001, p 127-134
152. A. Agüero, F.J. García de Blas, M.C. García, R. Muelas, and A. Román, Thermal Spray Coatings for Molten Carbonate Fuel Cells Separator Plates. Surf. Coat.Technol, 146-147, p 578-585 (2001)
153. R. Gonzalez, H. Ashrafizadeh, A. Lopera, P. Mertiny, and A. McDonald, A Review of Thermal Spray Metallization of Polymer-Based Structures, *J. Therm. Spray Technol.*, 2016, **25**(5), p 897-919.
154. K. Bobzin, W. Wietheger, and M.A. Knoch, Development of Thermal Spray Processes for Depositing Coatings on Thermoplastics, *J. Therm. Spray Technol.*, 2021, **30**(1), p 157-167.
155. A. Ranjan, A. Islam, M. Pathak, M.K. Khan, and A.K. Keshri, Plasma Sprayed Copper Coatings for Improved Surface and Mechanical Properties, *Vacuum*, 2019, **168**, p 108834.
156. S. Tailor, A. Modi, and S. Modi, Thermally Sprayed Thin Copper Coatings by W-HVOF, *J. Therm. Spray Technol.*, 2019, **28**(1), p 273-282.
157. N.A. Hamid, S. Wennig, S. Hardt, A. Heinzel, C. Schulz, and H. Wiggers, High-Capacity Cathodes for Lithium-Ion Batteries from Nanostructured $LiFePO_4$ Synthesized by Highly-Flexible and Scalable Flame Spray Pyrolysis, *J. Power. Sources*, 2012, **216**, p 76-83.
158. J. Joseph, A.T. Murdock, D.H. Seo, Z.J. Han, A.P. O'Mullane, and K. Ostrikov, Plasma Enabled Synthesis and Processing of Materials for Lithium-Ion Batteries, *Adv. Mater. Technol.*, 2018, **3**(9), p 1800070.
159. J. Nava-Avendaño and J. Veilleux, Plasma Processes in the Preparation of Lithium-Ion Battery Electrodes and Separators, *J. Phys. D Appl. Phys.*, 2017, **50**(16), p 163001.
160. S. Bhattacharjee, Y. Srivastava, V. Reghu, and P. Ramaswamy, Spray Dried Nano Oxide Ceramics for Free Flowing Plasma Spray Coating Powders and Battery Material Processing, *J. Phys.*, 2020, **1706**, p 012218.
161. X. Liang, Y. Wang, X. Zhang, D. Han, L. Lan, and Y. Zhang, Performance Study of a $Li_4Ti_5O_{12}$ Electrode for Lithium Batteries Prepared by Atmospheric Plasma Spraying, *Ceram. Int.*, 2019, **45**(17), p 23750-23755.
162. X. Wu, X. Liang, X. Zhang, L. Lan, S. Li, and Q. Gai, Structural Evolution of Plasma Sprayed Amorphous $Li_4Ti_5O_{12}$ Electrode and Ceramic/Polymer Composite Electrolyte during Electrochemical Cycle of Quasi-Solid-State Lithium Battery, *J. Adv. Ceram.*, 2021, **10**(2), p 347-354.
163. A. Hasani, A. Salminen, S. Joshi, M.G. Makowska, B. Chameh, V.-P. Lehto, V. Gidla, S. Goel, I. Angervo, and A. Ganvir, Process-Dependent Phase Evolution in Thermally Sprayed Li4Ti5O12 Thin-Film Anodes Revealed by Synchrotron and Surface Analysis, *Mater. Des.*, 2026 https://doi.org/10.1016/j.matdes.2026.116414
164. T.-H. Hsueh, C.-H. Tsai, S.-E. Liu, M.-C. Wang, S.-M. Chang, A. Shiue, and K.-Y. Chin, $LiCoO_2$ Battery Electrode Fabricated by High Deposition-Rate Atmospheric Plasma Spraying for Lithium Battery, *J. Electrochem. Soc.*, 2022, **169**(10), p 100506.
165. S.-L. Zhang, C.-X. Li, C.-J. Li, G.-J. Yang, and M. Liu, Application of High Velocity Oxygen Fuel Flame (HVOF) Spraying to Fabrication of La0.8Sr0.2Ga0.8Mg0.2O3 Electrolyte for Solid Oxide Fuel Cells, *J. Power. Sources*, 2016, **301**, p 62-71.
166. S. Singh, N. Nawbuntud, K. Khantisopon, A. Meghwal, J. Tharajak, P. Nawarat, C.C. Berndt, and A.S.M. Ang, Innovative Manufacturing of Nanostructured Solid State Electrolyte Using

Suspension Plasma Spray, *Surf. Coat. Technol.*, 2025, **507**, p 132112.
167. Y.-Q. Sun, X.-T. Luo, Y.-S. Zhu, X.-J. Liao, and C.-J. Li, Li_3PO_4 Electrolyte of High Conductivity for All-Solid-State Lithium Battery Prepared by Plasma Spray, *J. Eur. Ceram. Soc.*, 2022, **42**(10), p 4239-4247.
168. M. Ahmed, A.Z. Yazdi, S.B. Dayani, H. Jahed, and P. Chen, Fabrication of Zinc Anodes for Aqueous Lithium-Ion Batteries by Supersonic Cold Spraying, *ChemElectroChem*, 2019, **6**(5), p 1333-1337.
169. G. Vinay, N.M. Chavan, S. Kumar, A. Jyothirmayi, and B.R. Bodapati, Improved Microstructure and Properties of Cold Sprayed Zinc Coatings in the as Sprayed Condition, *Surf. Coat. Technol.*, 2022, **438**, p 128392.
170. A. Hasani, C. Nayak, G. Vinay, A. Salminen, S. Joshi, S. Goel, V. Gopal, E. Makila, M. Juan, and A. Ganvir, Laser Post-processing as a Surface Engineering Strategy for Atmospheric Plasma-Sprayed Thin-Film All-Solid-State Battery Components, *Appl. Surf. Sci.*, 2026, **735**, p 166624.
171. M. Ockel, A. Borchers, J. Fröhlich, M. Petersen, T. Paschen, S. Christiansen, and J. Franke, Atmospheric Plasma Spraying for Copper Coating of Ceramic Solid Electrolytes for Anode-Free Solid-State Batteries with Increased Interfacial Contact, 2024 1st International Conference on Production Technologies and Systems for E-Mobility (EPTS), IEEE, 2024, p 1-5
172. A.M. Laptev, H. Zheng, M. Bram, M. Finsterbusch, and O. Guillon, High-Pressure Field Assisted Sintering of Half-Cell for All-Solid-State Battery, *Mater. Lett.*, 2019, **247**, p 155-158.
173. C. Jiang and Y. Luo, Fabrication and Electrochemical Performance of YSZ-Based Metal-Supported SOFCs via High-Energy Atmospheric Plasma Spraying, *Ceram. Int.*, 2026 https://doi.org/10.1016/j.ceramint.2026.02.253
174. R. Hui, Z. Wang, O. Kesler, L. Rose, J. Jankovic, S. Yick, R. Maric, and D. Ghosh, Thermal Plasma Spraying for SOFCs: Applications, Potential Advantages, and Challenges, *J. Power. Sources*, 2007, **170**(2), p 308-323.
175. G. Schiller, R.H. Henne, M. Lang, R. Ruckdäschel, and S. Schaper, Development of Vacuum Plasma Sprayed Thin-Film SOFC for Reduced Operating Temperature, *Fuel Cells Bull.*, 2000, **3**(21), p 7-12.
176. D. Stöver, D. Hathiramani, R. Vaßen, and R.J. Damani, Plasma_Sprayed Components for SOFC Applications, *Surf. Coat. Technol.*, 2006, **201**(5), p 2002-2005.
177. P. Coddet, H.-l Liao, and C. Coddet, A Review on High Power SOFC Electrolyte Layer Manufacturing Using Thermal Spray and Physical Vapour Deposition Technologies, *Adv. Manuf.*, 2014, **2**(3), p 212-221.
178. C.-J. Li, C.-X. Li, Y.-Z. Xing, M. Gao, and G.-J. Yang, Influence of YSZ Electrolyte Thickness on the Characteristics of Plasma-Sprayed Cermet Supported Tubular SOFC, *Solid State Ionics*, 2006, **177**(19-25), p 2065-2069.
179. S.-F. Yang, C.-S. Hwang, C.-H. Tsai, C.-L. Chang, and M.-H. Wu, Production of Metal-Supported Solid Oxide Fuel Cell Using Thermal Plasma Spraying Technique, *IEEE Trans. Plasma Sci.*, 2016, **45**(2), p 318-322.
180. S.-L. Zhang, H.-X. Yu, C.-X. Li, S.Y. Lai, C.-J. Li, G.-J. Yang, H.-B. Sun, T. Wei, and M. Liu, Thermally Sprayed High-Performance Porous Metal-Supported Solid Oxide Fuel Cells with Nanostructured La 0.6 Sr 0.4 Co 0.2 Fe 0.8 O 3− δ Cathodes, *J. Mater. Chem. A*, 2016, **4**(19), p 7461-7468.
181. M. Vardavoulias, P. Gkomoza, M. Arkas, D.K. Niakolas, and S.G. Neophytides, Thermal Spray Multilayer Ceramic Structures with Potential for Solid Oxide Cell Applications, *Coatings*, 2021, **11**(6), p 682.
182. C. Nayak, A. Hasani, G. Vinay, E. Mäkilä, E. Owusu, N. Kamboj, M.G. Makowska, A. Lynam, A.R. Romero, and S. Goel, High-Resolution Synchrotron μXRD and μXRF for Local Phase and Elemental Analysis in Suspension Plasma Sprayed Environmental Barrier Coatings, *J. Therm. Spray Technol.*, 2026, **35**, p 1-13.
183. Y. Xiang, X. Li, Y. Cheng, X. Sun, and Y. Yang, Advanced Characterization Techniques for Solid State Lithium Battery Research, *Mater. Today*, 2020, **36**, p 139-157.
184. S. Liang, Y. Sun, Y.J. Cheng, S.V. Roth, P. Müller-Buschbaum, L. Cao, J. Peng, S. Wang, X. Sun, and C. Wang, Probing All-Solid-State Batteries with Real-Time Synchrotron and Neutron Techniques, *Adv. Energy Mater.*, 2026, **16**(5), p e04045.
185. E. Novak, L. Daemen, and N. Jalarvo, Advanced Characterization of Solid-State Battery Materials Using Neutron Scattering Techniques, *Materials*, 2024, **17**(24), p 6209.
186. K.L. Browning, A.S. Westover, J.F. Browning, M. Doucet, R.L. Sacci, and G.M. Veith, In Situ Measurement of Buried Electrolyte–Electrode Interfaces for Solid State Batteries with Nanometer Level Precision, *ACS Energy Lett.*, 2023, **8**(4), p 1985-1991.
187. E.D. Rus and J.A. Dura, In Situ Neutron Reflectometry Study of a Tungsten Oxide/Li-Ion Battery Electrolyte Interface, *ACS Appl. Mater. Interfaces*, 2023, **15**(2), p 2832-2842.
188. G.M. Veith, M. Doucet, J.K. Baldwin, R.L. Sacci, T.M. Fears, Y. Wang, and J.F. Browning, Direct Determination of Solid-Electrolyte Interphase Thickness and Composition as a Function of State of Charge on a Silicon Anode, *J. Phys. Chem. C*, 2015, **119**(35), p 20339-20349.
189. J.F. Browning, L. Baggetto, K.L. Jungjohann, Y. Wang, W.E. Tenhaeff, J.K. Keum, D.L. Wood III., and G.M. Veith, In Situ Determination of the Liquid/Solid Interface Thickness and Composition for the Li Ion Cathode $LiMn_{1.5}Ni_{0.5}O_4$, *ACS Appl. Mater. Interfaces*, 2014, **6**(21), p 18569-18576.
190. X. Zhang, M. Osenberg, R.F. Ziesche, Z. Yu, J. Kowal, K. Dong, Y. Lu, and I. Manke, Visualizing the Future: Recent Progress and Challenges on Advanced Imaging Characterization for All-Solid-State Batteries, *ACS Energy Lett.*, 2024, **10**(1), p 496-525.
191. A. Tang, M. Li, X. Sun, and W. Li, Interfacial Characterization in Solid-State Lithium Metal Batteries: Advances in Temporal, Spatial, and Energy Resolution, *Energy Environ. Sci.*, 2026 https://doi.org/10.1039/D5EE05519A
192. Y. Fu, G. Shao, and Y. Lei, Interface Engineering in Solid-State Sodium Batteries: Advances in Materials Design, Interfacial Strategies, and Multiscale Characterization, *Interdiscip. Mater.*, 2026, **5**(1), p 5-84.
193. D. Lou, H. Hong, M. Ellingsen, and R. Hrabe, Supersonic Cold-Sprayed Si Composite Alloy as Anode for Li-Ion Batteries, *Appl. Phys. Lett.*, 2023 https://doi.org/10.1063/5.0135408
194. A. Hasani, M. Luya, N. Kamboj, C. Nayak, S. Joshi, A. Salminen, S. Goel, and A. Ganvir, Laser Processing of Liquid Feedstock Plasma-Sprayed Lithium Titanium Oxide Solid-State-Battery Electrode, *Coatings*, 2024, **14**(2), p 224.
195. A. Lanzutti, F. Sordetti, E. Marin, F. Andreatta, A. Carabillo, M. Querini, S. Porro, A. Rondinella, M. Magnan, and L. Fedrizzi, The Use of Thin Films as Defect Sealants to Increase the Corrosion Resistance of Thermal Spray Coatings, *Metals*, 2023, **13**(10), p 1778.
196. G. Vinay, R. Kant, A. Piiroinen, C. Nayak, A. Ganvir, and H. Singh, Enhancing Cold-Sprayed Nickel-Aluminum Bronze Coatings on Magnesium via Scanner-Based Laser Remelting, *J. Therm. Spray Technol.*, 2026, **35**, p 1-19.
197. W. Huang, B. Zou, Y. Zhao, X. Meng, C. Wang, X. Cao, and Z. Wang, Fabrication of Novel Thermal Barrier Coating on Polymer Composites via the Combined Sol–Gel/Sealing Treatment Process, *Appl. Surf. Sci.*, 2012, **258**(22), p 9058-9066.

198. T. Van Nguyen, T.A. Nguyen, H.T. Pham, L.T. Pham, P.T. Nguyen, T.B. Dao, T. Van Trinh, D. Vu, and Q.T. Le, Sealing Treatment of Plasma-Sprayed Cr3C2-NiCr/Al2O3-TiO2 Coating by Aluminum Phosphate Sealant Containing Al2O3 Nanoparticles, *J. Therm. Spray Technol.*, 2022, **31**(1), p 269-281.
199. C.M. Rost, E. Sachet, T. Borman, A. Moballegh, E.C. Dickey, D. Hou, J.L. Jones, S. Curtarolo, and J.-P. Maria, Entropy-Stabilized Oxides, *Nat. Commun.*, 2015, **6**(1), p 8485.
200. A. Sarkar, L. Velasco, D. Wang, Q. Wang, G. Talasila, L. de Biasi, C. Kübel, T. Brezesinski, S.S. Bhattacharya, and H. Hahn, High Entropy Oxides for Reversible Energy Storage, *Nat. Commun.*, 2018, **9**(1), p 3400.
201. A. Anupam and S. Joshi, High Entropy Oxides as Next-Generation Thermal Barrier Coatings–a Processing Perspective, *J. Eur. Ceram. Soc.*, 2026 https://doi.org/10.1016/j.jeurceramsoc.2026.118499
202. P. Mahendru, M. Tembely, and A. Dolatabadi, Artificial Intelligence Models for Analyzing Thermally Sprayed Functional Coatings, *J. Therm. Spray Technol.*, 2023, **32**(2), p 388-400.
203. K. Bobzin, W. Wietheger, H. Heinemann, S. Dokhanchi, M. Rom, and G. Visconti, Prediction of Particle Properties in Plasma Spraying Based on Machine Learning, *J. Therm. Spray Technol.*, 2021, **30**(7), p 1751-1764.
204. D. Sun, Q. He, and Z. Huang, Machine Learning-Based Diagnosis of Thermal Barrier Coating Process Quality, *J. Therm. Spray Technol.*, 2024, **33**(5), p 1308-1323.
205. W. Li, H. Wu, X. Chu, Y. Xie, S. Deng, and S. Bagherifard, Outlook of Industry 4.0 Integrated Technologies in Thermal Spray Processes and Applications, *J. Therm. Spray Technol.*, 2025, **34**, p 1-30.

Publisher's Note Springer Nature remains neutral with regard to jurisdictional claims in published maps and institutional affiliations.